



Government of **Western Australia**
Department of **Mines and Petroleum**

RECORD 2009/6

MINERALOGY AND TRACE ELEMENT CHEMISTRY OF LODGE AND ALLUVIAL GOLD FROM THE WESTERN CAPRICORN OROGEN

by
EA Hancock, AM Thorne, PA Morris, RJ Watling¹, and
HNC Cutten

¹ Centre for Forensic Science, The University of Western Australia,
35 Stirling Highway, Crawley, WA, 6009, Australia



Geological Survey of Western Australia



**Government of Western Australia
Department of Mines and Petroleum**

Record 2009/6

MINERALOGY AND TRACE ELEMENT CHEMISTRY OF LODGE AND ALLUVIAL GOLD FROM THE WESTERN CAPRICORN OROGEN

by

EA Hancock, AM Thorne, PA Morris, RJ Watling¹, and HNC Cutten

¹ Centre for Forensic Science, The University of Western Australia, 35 Stirling Highway, Crawley, WA, 6009, Australia



**Geological Survey of
Western Australia**

**MINISTER FOR MINES AND PETROLEUM
Hon. Norman Moore MLC**

**DIRECTOR GENERAL, DEPARTMENT OF MINES AND PETROLEUM
Richard Sellers**

**EXECUTIVE DIRECTOR, GEOLOGICAL SURVEY OF WESTERN AUSTRALIA
Tim Griffin**

REFERENCE

The recommended reference for this publication is:

Hancock, EA, Thorne, AM, Morris, PA, Watling, RJ and Cutten, HNC 2009, Mineralogy and trace element chemistry of lode and alluvial gold from the western Capricorn Orogen: Geological Survey of Western Australia, Record 2009/6, 30p.

National Library of Australia Card Number and ISBN 978-1-74168-241-0 (PDF)

Grid references in this publication refer to the Geocentric Datum of Australia 1994 (GDA94). Locations mentioned in the text are referenced using Map Grid Australia (MGA) coordinates, Zone 50. All locations are quoted to at least the nearest 100 m.

Published 2009 by Geological Survey of Western Australia

This Record is published in digital format (PDF) and is available online at www.dmp.wa.gov.au/GSWApublications. Laser-printed copies can be ordered from the Information Centre for the cost of printing and binding.

Further details of geological publications and maps produced by the Geological Survey of Western Australia are available from:

Information Centre
Department of Mines and Petroleum
100 Plain Street
EAST PERTH, WESTERN AUSTRALIA 6004
Telephone: +61 8 9222 3459 Facsimile: +61 8 9222 3444
www.dmp.wa.gov.au/GSWApublications

Contents

Abstract	1
Introduction	1
Geological background	2
Mineralization	3
Study area geology and sample location	3
Egerton MC	3
Sample location	3
Low Hill	3
Sample location	4
Bangemall MC	4
Sample location	6
Star of Mangaroon MC	6
Sample location	7
Sampling and analytical methodology	7
Sampling method	7
Sample processing	7
Bedrock material	7
Placer material	7
Gold grains	7
Geochemical analysis	7
Assay method	7
SEM-EDX method	8
LA-ICP-MS analysis	8
Recovered gold	8
Egerton MC	8
Low Hill	8
Bangemall MC	8
Gold mineralogy	8
Egerton MC	8
Hibernian	8
Gaffney Find	20
Low Hill	20
Bangemall MC	22
Cobra	22
McCarthy's Patch	22
Gold geochemistry	23
SEM-EDX results	23
LA-ICP-MS results	23
Principal Components Analysis	24
Discussion	26
Regional variation in gold mineralogy and chemistry	26
Egerton MC	26
Low Hill	26
Bangemall MC	26
Gold mineralization history	27
Conclusions	27
Acknowledgements	27
References	28

Appendices

Laser Ablation (LA-ICP-MS) analysis	30
---	----

Figures

1. Simplified geological map of the Capricorn Orogen, showing the areas sampled during this study.....	2
2. Geological map of the Egerton Mining Centre	5
3. Geological map of the Low Hill area	5
4. Geological map of the Bangemall Mining Centre	6
5. Plot of covariance versus average counts per second for Laser Ablation-Inductively Coupled Plasma-Mass Spectroscopy (LA-ICP-MS) of standard reference materials Glass NIST 610 and Gold AUSTD1	18
6. Scanning Electron Microscope Back-Scattered Electron image of alluvial gold from Hibernian.....	18
7. Scanning Electron Microscope Back-Scattered Electron image of lode gold from Gaffney Find	18
8. Scanning Electron Microscope Back-Scattered Electron image of well-rounded alluvial gold grains with pitted surface from Gaffney Find	18
9. Distribution of gold flakes in variscite matrix from Low Hill.....	18
10. Scanning Electron Microscope Back-Scattered Electron image of lode gold from Cobra.....	19
11. Scanning Electron Microscope Back-Scattered Electron image of alluvial gold from Carthys Patch	19
12. Scanning Electron Microscope Back-Scattered Electron images showing the diversity of gold morphology from Hibernian	19
13. Internal structure of a Hibernian gold grain showing coherent twins and high-purity segregations	20
14. Scanning Electron Microscope Back-Scattered Electron image of solid, cemented lode gold grain from Gaffney Find.....	20
15. Internal structure of Gaffney Find lode gold grain showing recrystallization, incoherent curved twins, intergranular veinlets, and a high-purity segregation	20
16. Scanning Electron Microscope Back-Scattered Electron image of spongy secondary gold in variscite at Low Hill.....	21
17. Scanning Electron Microscope Back-Scattered Electron image of a gold, goethite, and quartz assemblage at Cobra.....	21
18. Scanning Electron Microscope Back-Scattered Electron image of variations in morphology of lode gold grains from Cobra.....	21
19. Internal structure of a Cobra lode gold grain showing areas of initial recrystallization on the grain margin	22
20. Internal structure of a Cobra lode gold grain showing high-purity intergranular veinlets.....	22
21. Well-rounded alluvial gold grain with a pitted surface from McCarthys Patch.....	22
22. Internal structure of an alluvial gold grain from McCarthys Patch, showing high-purity intergranular veinlets and irregular corrosive rim.....	22
23. Spiderdiagrams showing the variations in siderophile (Ti–Ni) and chalcophile (Cu–Bi) elements for gold analysed by Laser Ablation-Inductively Coupled Plasma-Mass Spectroscopy (LA-ICP-MS)	23
24. Bivariate element plots showing variation in silver versus copper; lead versus mercury; antimony versus mercury	24
25. Bivariate element plots showing variation in iron versus manganese and vanadium versus cobalt.....	25
26. Principal Components Analysis for the sample series 149047 and 149057, based on copper, silver, antimony and mercury.....	25
27. Principal Components Analysis for the sample series 149070 and 149074, based on copper, silver, antimony, and mercury	25
28. Principal Components Analysis for the complete Capricorn sample series, based on copper, silver, and mercury.....	25
29. Principal Components Analysis for the sample series 149047 and 149057, showing differences between lithogenic elemental associations.....	25

Tables

1. Sample location, assay results, and number of gold particles recovered from the Hibernian, Gaffney Find, Low Hill, Cobra, McCarthys Patch, and Mangaroon localities	4
2. Summary of mineralogical and geochemical characteristics of lode and alluvial gold recovered from the Hibernian, Gaffney Find, Low Hill, Cobra, and McCarthys Patch localities.....	9
3. Laser Ablation-Inductively Coupled Plasma-Mass Spectroscopy (LA-ICP-MS) data for gold from the Hibernian, Gaffney Find, Low Hill, Cobra, and McCarthys Patch localities.....	10
4. Laser Ablation-Inductively Coupled Plasma-Mass Spectroscopy (LA-ICP-MS) data for reference samples Glass NIST 610, and Gold AUSTD1.....	16

Mineralogy and trace element chemistry of lode and alluvial gold from the western Capricorn Orogen

by

EA Hancock, AM Thorne, PA Morris, RJ Watling¹, and HNC Cutten

Abstract

Gold grains from the Egerton Mining Centre, Bangemall Mining Centre, and Low Hill were examined in terms of their size, morphology, silver content, trace element distribution, and internal structure. Chemical data were obtained using a Scanning Electron Microscope with Energy Dispersive X-ray system (SEM-EDX) and through Laser Ablation-Inductively Coupled Plasma-Mass Spectrometry (LA-ICP-MS). Principal Components Analysis (PCA) was applied to support mineralogical observations and chemical results.

Lode and alluvial gold from the Egerton Mining Centre, associated with low-grade Paleoproterozoic metasedimentary rocks of the Padbury Group, are all similar in chemistry, and are characterized by their low silver concentrations, high copper to silver ratios, low mercury to lead ratios, the presence of recrystallized twinning, high-purity segregations, and intergranular silver depletion. All of these features are characteristic of a relatively high-pressure and high-temperature hypogene origin with significant secondary alteration. At least two populations of alluvial gold are present at the Egerton Mining Centre, derived from separate sources.

Lode and alluvial gold grains of the Bangemall Mining Centre, associated with Mesoproterozoic dolerite and very low-grade sedimentary rocks of the Edmund Group, differ from gold sampled from the Egerton Mining Centre in their association with relatively unweathered pyrite and milky quartz; higher silver, mercury, and antimony content; and relatively simple, monocrystalline internal structure. These features are consistent with primary mineralization in a slightly oxidized, non-lateritic environment, rather than in a deeper crustal, hypogenic setting. There is a single source for alluvial gold at the Bangemall Mining Centre. However, gold has likely undergone several transport cycles before being incorporated into the present-day alluvium.

Gold associated with variscite at Low Hill has a distinctive spongy morphology and very high purity. The gold flakes were probably formed by the remobilization and redeposition of stratiform gold by low-temperature, saline solutions in a supergene environment.

This work indicates that the Capricorn Orogen underwent at least two periods of hydrothermal gold mineralization during the Proterozoic, and at least one period of secondary gold formation, probably during the Phanerozoic.

KEYWORDS: Lode gold, alluvial gold, gold mineralogy, gold chemistry, Capricorn Orogen, SEM-EDX, LA-ICP-MS, Principal Components Analysis, Egerton Mining Centre, Bangemall Mining Centre, Low Hill, variscite.

Introduction

Gold mineralogy and geochemistry have been used successfully in exploration for gold for more than a half century. Studies of gold from different geological and climatic provinces have provided information on the original sources of gold mineralization, the physical and chemical conditions of mineralizing systems, the tectonic and metamorphic history of the deposits, and their supergene alteration (Petrovskaya, 1973; Boyle, 1979; Knight et al., 1999; Chapman et al., 2002; Nikolaeva et al., 2004; Freyssinet et al., 2005).

The northwestern Capricorn Orogen of central Western Australia contains a number of small, gold-bearing

hydrothermal veins that are found in a variety of geological settings. These include low-grade Paleoproterozoic pelitic, psammitic, and mafic schist of the Padbury Group at the Egerton Mining Centre; Mesoproterozoic dolerite and Edmund Group sediments at the Bangemall Mining Centre; Late Paleoproterozoic migmatite of the Pooranoo Metamorphics, and granite of the Durlacher Supersuite at the Star of Mangaroon site; and vein and stratabound gold mineralization associated with variscite in the Edmund Group at Low Hill.

This study examines gold mineralogy and trace element chemistry from different deposits in the Capricorn Orogen to determine if they result from related mineralization events. A further objective was to determine the extent to which these properties have been modified by subsequent processes, such as gold remobilization and weathering. In this study, gold was characterized using parameters

¹ Centre for Forensic Science, The University of Western Australia, 35 Stirling Highway, Crawley, WA, 6009, Australia

including size, morphology, and, where possible, internal structure. Silver content was determined using a Scanning Electron Microscope with Energy Dispersive X-ray system (SEM-EDX). These results were supplemented by information on the trace element signature of the gold, obtained from Laser Ablation-Inductively Coupled Plasma-Mass Spectrometry (LA-ICP-MS) analyses.

Geological background

The study area is situated in the western part of the Capricorn Orogen, a major zone of Proterozoic deformation, metamorphism, and magmatism lying between two Archean cratons — the Yilgarn Craton to the south and the Pilbara Craton to the north (Gee, 1979; Cawood and Tyler, 2004; Fig. 1). The orogen includes metamorphic and igneous rocks of the Gascoyne Province, a number of sedimentary basins, and the deformed margins of the neighbouring cratons. Within the study area, the Capricorn Orogen comprises Paleoproterozoic rocks of the Padbury Basin and Gascoyne Province, and Late Paleoproterozoic to Mesoproterozoic rocks of the Edmund Basin (Fig. 1).

The Padbury Basin is one of the three basins previously included in the former Glengarry Basin (Pirajno et al., 1996). Sedimentary and volcanic rocks in these basins

were deposited and deformed along the northern margin of the Yilgarn Craton sometime between 2.0 and 1.65 Ga (Gee, 1990; Cawood and Tyler, 2004), although these ages are not well constrained. Within the Padbury Basin, the Padbury Group (Occhipinti et al., 1996; Swager and Myers, 1999; Sheppard and Swager, 1999) contains mineral assemblages indicative of greenschist-facies metamorphism (Swager and Myers, 1999).

The Gascoyne Province is composed of Paleoproterozoic metasedimentary and meta-igneous rocks, extensively intruded by large volumes of granite. The southern part of the Gascoyne Province comprises late Archean to Paleoproterozoic foliated and gneissic granitic and metasedimentary rocks, collectively referred to as the Glenburgh Terrane (Sheppard, 2004). The Paleoproterozoic geology of the northern Gascoyne Province can also be described in terms of three zones: the Boora Boora, Mangaroon, and Limejuice Zones. Most of the Gascoyne Province rocks in the study area belong to the Mangaroon Zone, which consists of sedimentary rocks deposited after c. 1680 Ma, immediately prior to deformation and metamorphism at medium- to high-grade during the Mangaroon Orogeny at 1680–1620 Ma (Sheppard et al., 2005). These metamorphic rocks form part of the Pooranoo Metamorphics. Granite plutons of the Durlacher Supersuite were largely intruded into the Pooranoo Metamorphics at 1680–1660 Ma during, and shortly after, the peak of regional metamorphism (Martin et al., 2005; Sheppard et al., 2005).

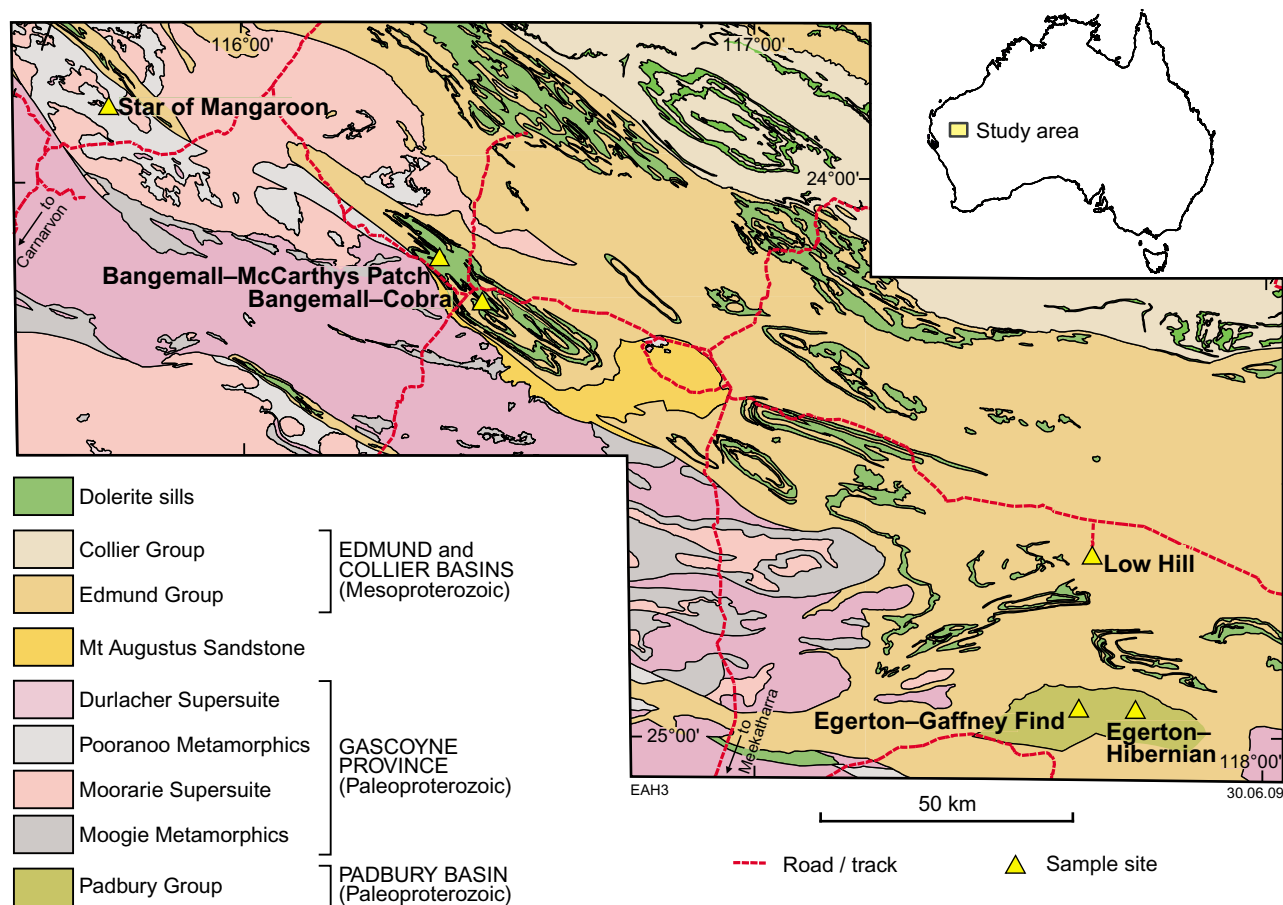


Figure 1. Simplified geological map of the Capricorn Orogen, showing the areas sampled during this study.

The Edmund Basin is the second youngest tectonic unit within the Capricorn Orogen, with a geographic extent that corresponds to the present-day outcrop of the Edmund Group (lower Bangemall Supergroup). The Edmund Group comprises very low grade metasedimentary rocks (Martin et al., 2005), although Sheppard et al. (2008) describe the effects of greenschist- to amphibolite-facies metamorphism on central MOUNT PHILLIPS*. The Edmund Group is younger than 1680–1620 Ma granites of the underlying Gascoyne Province, and older than c. 1465 Ma dolerite sills that intrude it over large areas of the Capricorn Orogen (Martin and Thorne, 2004).

Tyler and Thorne (1990), Myers (1993), and Krapez (1999) interpreted the Capricorn Orogen as the result of collision between the Pilbara and Yilgarn Cratons during the Paleoproterozoic. This interpretation has since been refined based on the results of recent mapping and geochronology studies from the Gascoyne Province and southern Pilbara, which have shown that the Capricorn Orogen underwent several tectonothermal events during the Paleoproterozoic, most importantly the c. 2200 Ma Ophthalmian Orogeny, the 2005–1950 Ma Glenburgh Orogeny, the 1830–1780 Ma Capricorn Orogeny, and the 1680–1620 Ma Mangaroon Orogeny (Cawood and Tyler, 2004; Kinny et al., 2004; Occhipinti et al., 2001; Sheppard et al., 2005). An important conclusion from this work is that the Glenburgh Terrane in the southern Gascoyne Province is allochthonous to both the Yilgarn and Pilbara Cratons, and collided with the Yilgarn Craton during the Glenburgh Orogeny (Occhipinti et al., 2004). Major tectonothermal events also affected the Capricorn Orogen during the Mesoproterozoic and Neoproterozoic. These include two periods of dolerite sill intrusion into the Edmund and Collier Groups, at around 1465 Ma and 1070 Ma respectively; the 1030–950 Ma Edmundian Orogeny; and the 550 Ma Mulka tectonic event (Sheppard et al., 2008).

Mineralization

Although the region has a history of mining dating back to the 1890s, there are few mines currently operating in the western Capricorn Orogen. The major mineral occurrences in this region have been documented by Cooper et al. (1998) and Hassan (2007).

Study area geology and sample location

Samples of mineralized bedrock and alluvium were collected from the Egerton, Bangemall, and Star of Mangaroon mining centres (herein referred to as the Egerton MC, Bangemall MC, and Star of Mangaroon MC, respectively), and from Low Hill (Fig. 1). The location of these samples is given in Table 1.

* Capitalized names refer to standard 1:100 000 map sheets, unless otherwise indicated.

Egerton MC

The Egerton MC (Figs 1 and 2) is located on south-central MOUNT EGERTON. The geology of this area has been described by Muhling et al. (1978), Dahl (1997), Cooper et al. (1998), and Brooklea Geoservices (1998), and the following description is based on these accounts.

Most of the gold mining in the Egerton MC took place between 1910 and 1953, with another short period of activity in 1983. The bulk of the gold has been collected from auriferous quartz veins, alluvial deposits, and mullock dumps at the Hibernian, Egerton, and Gaffney Find workings. Major exploration programs are summarized in Cooper et al. (1998), table 3.

Host rocks at the Egerton MC comprise low-grade pelitic and psammitic schist, interlayered with lesser amounts of mafic schist, and metadolostone. They unconformably underlie the basal Edmund Group and were correlated with the Glengarry (now Padbury) Group by Muhling et al. (1978) and Sheppard and Swager (1999). Mineralization at the Hibernian and Egerton workings is centred on quartz veins near the west-southwest trending contact between a thick, foliated metagabbro or metadolerite, and quartz–muscovite pelitic schist (Muhling et al., 1978; Dahl, 1997). Most other workings, including those at Gaffney Find, are centred on lenticular, pyritic quartz veins, aligned parallel to the foliation in the steeply dipping pelite and psammite host rocks.

Sample location

Bedrock and alluvial material were collected from the Hibernian workings, and from Gaffney Find, approximately 12 km to the west.

At Hibernian, GSWA samples 149044 and 149045 were taken from a saprolitic exposure of quartz-veined, steeply foliated, chloritic mafic schist, exposed in old workings (MGA 575716E 7241632N). Alluvial material was also collected from three creeks that drained the southwestern part of the Hibernian workings (GSWA samples 149040, 149041, 149042, 149043, 149069, and 149070; Table 1).

Two samples of bedrock material were collected from quartz veins and a quartz vein breccia, which cut foliated psammite and pelite at Gaffney Find (GSWA 149046, and 149047; Table 1). Samples of alluvium (GSWA 149048, 149049, and 149071) were also collected from small creeks draining these workings.

Low Hill

Finely disseminated gold is found within thin veins of cellular and massive variscite near Low Hill (Figs 1 and 3), on western MOUNT EGERTON (Nickel et al., 2008). The variscite veins cut north-dipping siltstone and fine-grained sandstone in the upper part of the Kiangi Creek Formation, middle Edmund Group (Martin et al., 2006). Within the study area, the Kiangi Creek Formation is open to tightly folded, mostly as a result of the 1030 Ma to 950 Ma Edmundian Orogeny, and intruded locally by 1465 Ma old

Table 1. Sample location, assay results, and number of gold particles recovered from the Hibernian, Gaffney Find, Low Hill, Cobra, McCarthys Patch, and Mangaroon localities

<i>Mining area</i>	<i>GSWA sample no.</i>	<i>Material type</i>	<i>Easting^(a)</i>	<i>Northing</i>	<i>Assay Au (ppb)</i>	<i>Assay Pt (ppb)</i>	<i>Assay Pd (ppb)</i>	<i>No. of gold particles recovered</i>
Egerton/Hibernian	149040	Placer	575863	7241378	1	<1	<1	0
Egerton/Hibernian	149041	Placer	575861	7241412	1	<1	<1	0
Egerton/Hibernian	149042	Placer	575767	7241491	12	<1	<1	0
Egerton/Hibernian	149043/149070	Placer	575681	7241474	211	<1	<1	19
Egerton/Hibernian	149044	Bedrock	575716	7241632	1 200	2	2	0
Egerton/Hibernian	149045	Bedrock	575716	7241632	16	6	7	0
Egerton/Hibernian	149069	Placer	575970	7241736	–	–	–	0
Egerton/Gaffney	149046	Bedrock	563778	7240865	350	6	4	0
Egerton/Gaffney	149047	Bedrock	563778	7240865	1 040	3	3	8
Egerton/Gaffney	149048	Placer	563927	7241315	15	<1	<1	0
Egerton/Gaffney	149049	Placer	563904	7241378	3	<1	<1	0
Egerton/Gaffney	149071	Placer	563458	7240118	–	–	–	2
Low Hill	149050	Placer	566817	7272499	11	2	<1	0
Low Hill	149051	Placer	566802	7272466	10	3	2	0
Low Hill	149052	Placer	566942	7272477	6	2	<1	0
Low Hill	149053	Placer	566943	7272533	4	<1	<1	0
Bangemall/Cobra	149054	Bedrock	446670	7322136	390	<1	<1	0
Bangemall/Cobra	149055	Placer	446673	7322057	21	<1	<1	0
Bangemall/Cobra	149056	Placer	446624	7322052	17	<1	<1	0
Bangemall/Cobra	149057	Bedrock	445745	7322635	6 220	<1	<1	50
Bangemall/Cobra	149058	Placer	445412	7322946	18	<1	<1	0
Bangemall/Cobra	149059	Placer	445337	7323010	13	<1	<1	0
Bangemall/McCarthy	149060	Placer	436270	7331670	30	<1	<1	0
Bangemall/McCarthy	149061	Placer	436226	7331719	60	<1	<1	0
Bangemall/McCarthy	149062/149074	Placer	436263	7331675	–	–	–	21
Mangaroon (Pb)	149063	Bedrock	371615	7361088	209	<1	<1	0
Mangaroon (Pb)	149064	Placer	371618	7361027	3	<1	<1	0
Mangaroon (Pb)	149065	Placer	371556	7361021	3	<1	<1	0
Unnamed Mangaroon	149066	Bedrock	372257	7360668	62	5	3	0
Unnamed Mangaroon	149067	Placer	372341	7360718	13	<1	2	0
Unnamed Mangaroon	149068	Tailings	272344	7360710	9	2	6	0

NOTES: Assay data from LA-ICP-MS analyses carried out at Ultratrace Laboratories, Canning Vale, Western Australia. Detection limit: 1 ppb

(a) MGA Zone 50

sills of Narimbunna Dolerite (Martin et al., 2005, Sheppard et al., 2005). The variscite mineralization, which consists of several thin seams, is contained within a zone about 0.5 m thick, which can be traced in outcrop for at least a kilometre. Most seams are broadly conformable with the sedimentary layering, although one thicker, discordant vein, varying from 30 to 50 mm in thickness, cuts across the sedimentary succession at a low angle. This discordant vein also cuts across, and therefore post-dates, closely spaced jointing in Kiangi Creek Formation siltstone. The relationship between conformable seams and the thicker discordant vein is unclear due to limited exposure.

Sample location

The mineralogy and trace element chemistry of gold associated with variscite veining near Low Hill has

been described previously by Nickel et al. (2008), and additional bedrock material was not collected during the course of the present study. However, two small creeks that drain the northern outcrop of the variscite deposit (MGA 566940E 7272530N) were sampled for alluvial gold (GSWA samples 149050, 149051, 149052, and 149053; Table 1).

Bangemall MC

The Bangemall MC, located in an outlier of Edmund Group rocks on north-central MOUNT PHILLIPS (Figs 1 and 4), has an intermittent history of minor gold production dating back to 1896 (Williams et al., 1983). The principal workings occur in the area immediately south and southwest of Cobra Homestead, and 12 km to the northwest of this homestead at McCarthys Patch.

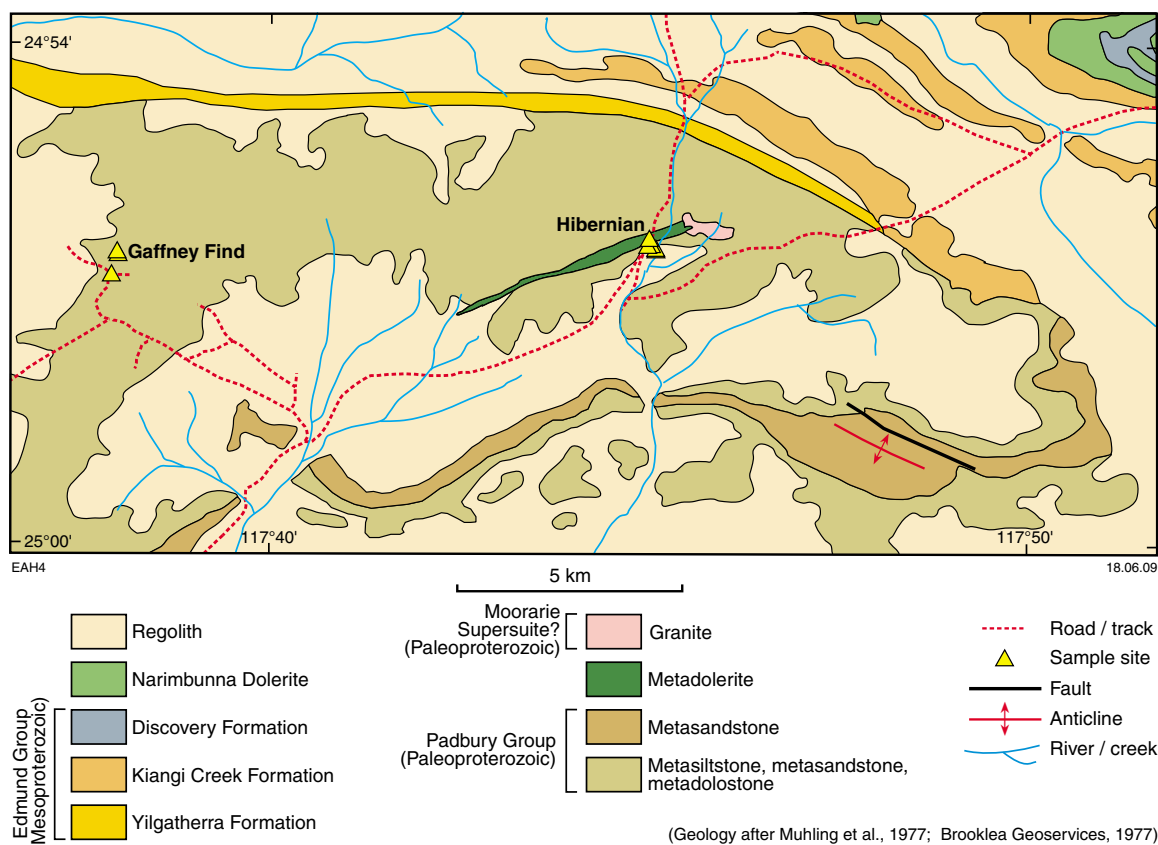


Figure 2. Geological map of the Egerton Mining Centre, showing the location of the Hibernian and Gaffney Find workings.

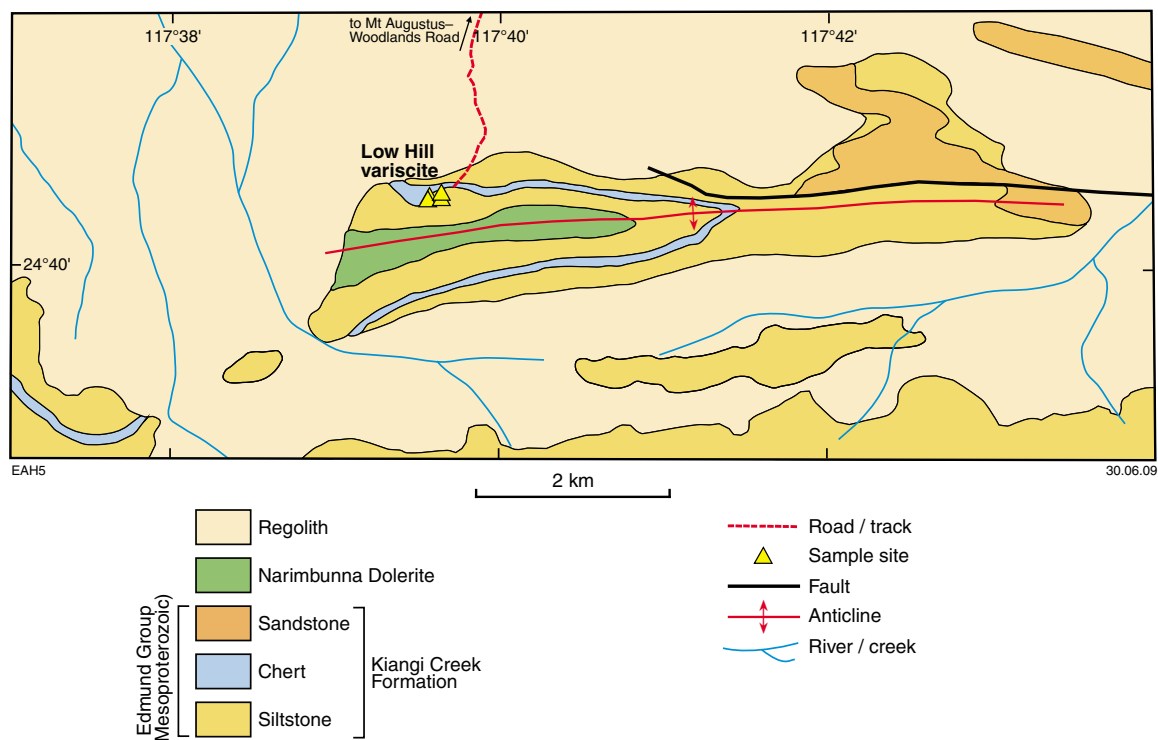


Figure 3. Geological map of the Low Hill area, showing the location of gold-bearing variscite workings.

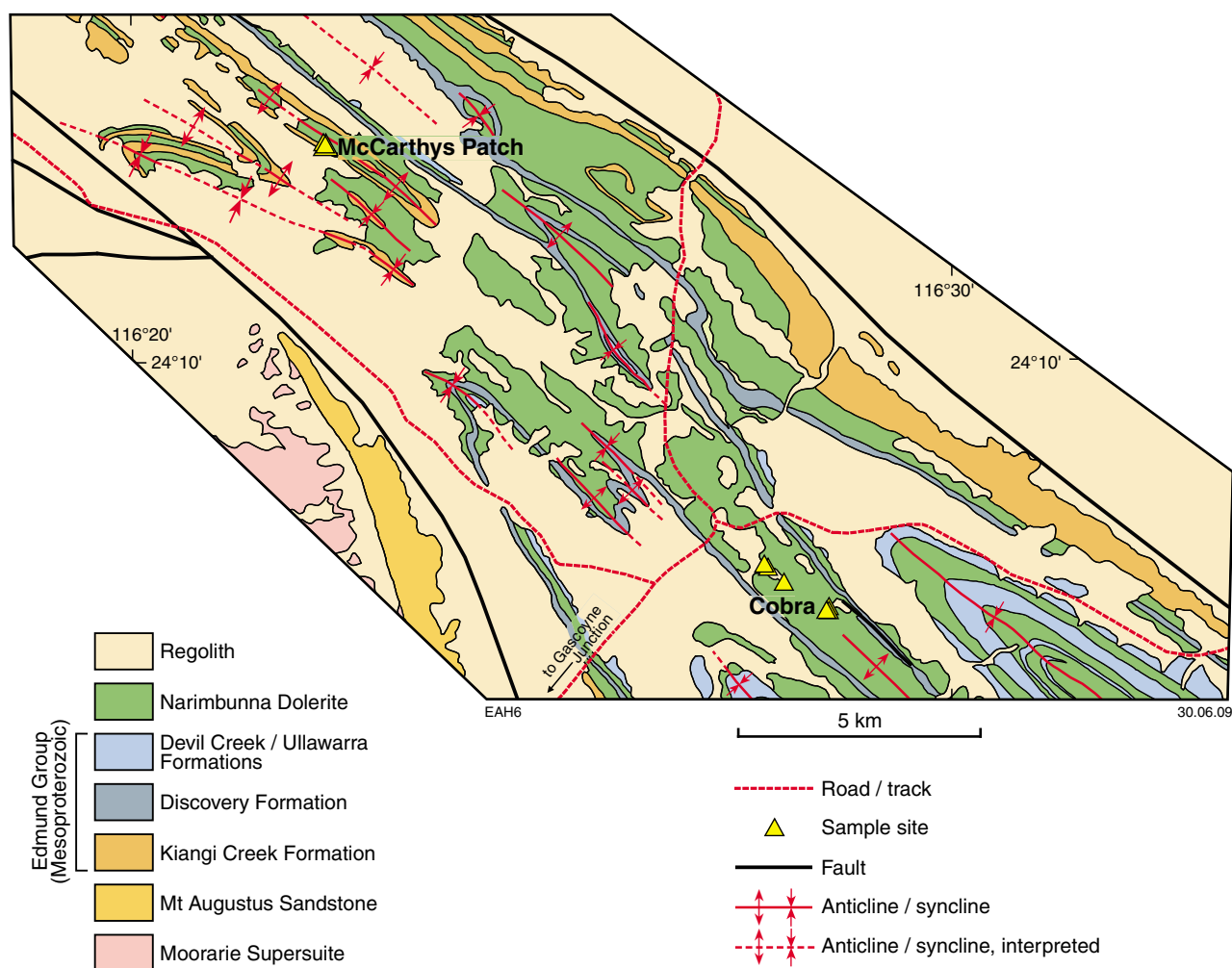


Figure 4. Geological map of the Bangemall Mining Centre, showing the location of the Cobra and McCarthys Patch workings.

The stratigraphic and structural settings for the Cobra and McCarthys Patch localities are similar. In both cases, gold is found within siltstone and sandstone of the Kiangi Creek Formation that has been extensively intruded by sills of the 1465 Ma Narimbunna Dolerite (Sheppard et al., 2008). Gold mineralization is associated with pyrite and carbonate, and occurs in quartz veins and stringers in the cores of tight, southeast-plunging anticlines (Williams et al., 1983). Most quartz veins dip steeply to the southwest or northeast, subparallel to the fold axial surfaces.

Sample location

Two samples of gossanous quartz vein material and four samples of alluvium were collected from the Cobra workings (Table 1). Quartz vein sample GSWA 149054 was collected from a spoil heap at the El Dorado workings (Cooper et al., 1998), and GSWA 149057 was taken from a 45° northward-dipping, brecciated, gossanous quartz vein that cuts interlayered saprolitic siltstone and dolerite near the Boss workings (Cooper et al., 1998). Two samples of alluvium (GSWA 149055, and 149056) were taken

from an east-southeast flowing creek near the El Dorado workings. Samples GSWA 149058 and 149059 were taken from alluvium in a northwesterly draining creek, 400 m northwest of the Boss workings.

Four samples of alluvium (GSWA 149060, 149061, 149062, and 149074) were collected from three sites at McCarthys Patch (Table 1), GSWA 149062 and 149074 being collected close to one another from the same sample location.

Star of Mangaroon MC

The Star of Mangaroon MC lies within the northwestern part of the Gascoyne Province on southwest EDMUND (1:250 000), and has a history of minor base metal and associated gold production dating back to 1956 (Blockley, 1971). The principal workings are at Star of Mangaroon, Star of Mangaroon South, and Mangaroon (Pb), although none of these mines are operating at present. Only Mangaroon (Pb), and unnamed workings located 750 m to the southeast of this locality, were visited during this study (Table 1). Descriptions of the

mineralization and host geology of the Star of Mangaroon area were provided by Blockley (1971) and Martin et al. (2005), and the following summary is based on these accounts.

At Mangaroon (Pb), lead mineralization is hosted in strongly sheared metasedimentary rocks of the c. 1680 Ma Pooranoo Metamorphics, and in weakly sheared biotite-bearing granite of the 1680–1620 Ma Durlacher Supersuite. Martin et al. (2005) noted that in this area the foliation strikes east-southeast and dips steeply to the north, whereas small-scale tight folds with S-vergence plunge shallowly to the southeast. This, together with an S–C fabric, suggests northeast-side up reverse faulting. Mining from 1956 to 1960 produced 11.61 t of concentrate, containing 8.43 t lead, 0.1418 t copper, 2923.6 g silver, and 1524 g gold (Blockley, 1971). Blockley (1971) reported that ore was mined from three en echelon quartz veins, which strike north and dip 10–15° to the east; that is, in a similar orientation to the vein system at the Star of Mangaroon workings.

Sample location

Sample GSWA 149063, composed of vein quartz with abundant galena and malachite, was collected from spoil heaps around the Mangaroon (Pb) workings (Table 1). Two samples of alluvium (GSWA 149064, and 149065) were also taken from the bed of an easterly flowing creek on the south side of the deposit.

A gently west-dipping quartz vein containing visible galena and malachite was sampled from workings 750 m to the southeast of Mangaroon (Pb) (Sample GSWA 149066; Table 1). Alluvium from the bed of a nearby southeasterly flowing creek (GSWA 149067), and sandy material from a tailings dump (GSWA 149068), was also collected.

Sampling and analytical methodology

Sampling method

Bedrock samples of approximately 10 kg were collected by hand from shallow pits or spoil heaps within the mine areas. A similar amount of alluvial sand and gravel were taken from dry creek beds that drained the prospect areas. Wherever possible, this material was collected from sediment traps that occurred close to the bedrock–alluvium contact.

Sample processing

The initial processing of bedrock and placer samples was undertaken in the laboratory, where the search for gold particles could be carried out under controlled conditions. A 500 g split of samples GSWA 149040–61 and GSWA 149063–68, was also submitted for gold assay; results are presented in Table 1.

Bedrock material

One kilogram of bedrock material was crushed and ground to less than 2 mm grain size. This material was then panned and dried, and the heavy mineral component was carefully examined for contained gold using an optical microscope. Gold grains and some of the associated heavy minerals were then mounted onto carbon adhesive tape for SEM imaging and analysis.

The variscite samples from Low Hill were crushed into small chips in an attempt to recover thin gold films for LA-ICP-MS analysis.

Using bedrock samples from Gaffney Find and Cobra, polished slabs were prepared in order to determine the textural relationships and paragenesis of the gold particles.

Placer material

Between one to ten kilograms of material was sieved from each alluvial sample, with the <2 mm size fraction panned and dried. Gold particles were recovered from the heavy mineral component and mounted as for bedrock gold.

A representative suite of heavy minerals were also mounted for SEM identification.

Gold grains

The gold and other heavy minerals recovered from the bedrock and placer samples were described mineralogically and photographed. In addition, the first round of SEM-EDX and Laser Ablation analyses were carried out on gold grains, using methodologies discussed more fully below. After this initial analysis, the gold grains were mounted in epoxy resin, sectioned, and polished, prior to being etched with aqua regia. This was followed by further optical work to determine the internal structure of the gold. A second round of SEM-EDX and LA-ICP-MS analysis was then conducted to compare the trace element chemistry of selected features in the gold microstructure.

Planned Electron Microprobe analysis of the gold could not be carried out in the time frame of this project because no working microprobe was available in Western Australia at the time.

Geochemical analysis

Assay method

Twenty eight samples were analysed for gold, palladium, and platinum by Ultratrace Laboratories (Canning Vale, Western Australia). Representative amounts of each sample were crushed, and then pulverized in a vibrating disc pulverizer. Precious metals were preconcentrated by lead-collection fire assay using approximately 40 g of sample pulp. The resulting prill was dissolved in acid, and gold, palladium, and platinum content determined by Inductively Coupled Plasma-Mass Spectrometry (ICP-MS). All twenty-eight samples were analysed in a single

batch, along with three reference materials. In addition, three samples were analysed in duplicate, and ten samples were analysed twice for the three target elements (i.e. replicate analysis). The lower level of detection for all three elements was 1 ppb. Excellent agreement was obtained on the analysed and defined values of the reference materials, and for the duplicate and replicate analysis of unknowns. Analytical results are shown in Table 1.

SEM-EDX method

The determination of silver content in gold grains, and the identification of heavy minerals, was achieved by SEM-EDX analysis, using a Philips XL-40 Scanning Electron Microscope at CSIRO, Kensington, Western Australia. This method provides semi-quantitative data with a detection limit of about 0.5%. Spot analyses were applied to selective gold grains before and after cutting; results showing the variation in silver content within the samples are presented in Table 2.

LA-ICP-MS analysis

LA-ICP-MS analysis of selected gold grains from five samples was carried out at the University of Western Australia, using an Agilent 7500CS ICP-MS system. Sample preparation, analytical conditions, and data reduction procedures are discussed in Appendix 1. The resulting data, for fifty-five elements between atomic mass 45 (scandium) and 238 (uranium) are reported in Table 3. All data are reported in counts per second (cps) rather than in terms of absolute concentrations (e.g. ppb), making the following discussions of element variation relative (Watling et al., 1994).

Analytical precision for the LA-ICP-MS method was assessed using the mean and covariance (i.e. 100SD/mean) of two analysed reference materials — glass NIST 610 and gold AUSTD1 (Table 4). For reference sample NIST 610 (Fig. 5a), covariance is close to 20 for elements at >1000 cps, although even some elements with the mean cps of <1000 (e.g. iridium) have low covariance values. For most elements in AUSTD1, the mean is <1000 cps (Fig. 5b), and the covariance is correspondingly higher (50–240). Data for both reference materials show an increase in covariance for most elements at about 1000 cps, which is taken as the likely upper level of background (i.e. threshold). As only two reference materials have been analysed, and concentrations are not available for both, data above the 1000 cps threshold are treated relatively.

Recovered gold

Gold was recovered from the Egerton MC, Bangemall MC, and Low Hill samples; however, no gold grains were recovered from the Star of Mangaroon workings (Table 1).

Egerton MC

Nineteen grains of placer gold (Fig. 6) were recovered from GSWA samples 149043 and 149070, both of

which were collected from the same (Table 1) short, southwest-draining creek near the southwestern extension of the Hibernian workings. No gold was recovered from the other four Hibernian alluvial samples or from the two bedrock samples collected in shallow workings at this site.

Small amounts of gold were recovered from Gaffney Find, with only eight grains of bedrock-hosted gold obtained from sample GSWA 149047 (Fig. 7), collected from brecciated quartz vein material in foliated psammite. In addition, two grains of placer gold were recovered from sample GSWA 149071 (Fig. 8), taken from alluvial material in a southwesterly flowing creek on the southeast side of the workings.

Low Hill

Samples of gold-bearing variscite (Fig. 9) from a massive variscite vein at Low Hill were provided for study by the prospect leaseholder, Mr. David Vaughan. No gold was recovered from alluvium in creeks draining the Low Hill workings (Table 1).

Bangemall MC

Fifty grains of gold were recovered from GSWA 149057 (Fig. 10), sampled from a brecciated, gossanous quartz vein at the Cobra workings (Table 1). In addition, twenty-one placer gold particles were extracted from GSWA samples 149062 and 149074, collected from McCarthys Patch (Fig. 11).

Gold mineralogy

The mineralogy of recovered gold is summarized in Table 2. Gold grains from each location were characterized in terms of their size, shape, degree of roundness, surface features, internal structure, silver concentration, and trace element levels.

Egerton MC

Hibernian

All Hibernian gold grains can be distinguished through their rich yellow colour. Individual grains range in size from 0.1 to 1.8 mm, with a mean value of 0.55 mm, and there is a wide diversity in grain morphology (Fig. 6). Well-rounded grains with even, smooth surfaces are most abundant (Fig. 12a), although some grains are slightly rounded with irregular cementing and semi-crystalline segregations, and intergrown with quartz, mica, and altered potassium-feldspar (Fig. 12b). Subrounded semi-idiomorphic, and lumpy grains with pitted and rugged surfaces, are also recorded (Fig. 12c).

Protracted leaching of gold grains in aqua regia for up to five minutes revealed internal structure in only two slightly rounded grains. They display simple coherent twins, partial

Table 2. Summary of mineralogical and geochemical characteristics of lode and alluvial gold recovered from the Hibernian, Gaffney Find, Low Hill, Cobra, and McCarthys Patch localities

Location	Number (GSWA)	Gold grains	Size mm (mean)	Shape	Surface	Roundness	Ag, wt%	Trace elements (>1000 cps)	Internal structure
Hibernian (alluvium)	149070 (149043)	19	0.1–1.8 (0.55)	Rounded cemented and semi-idiomorphic	Even, pitted, rugged	Sub-medium – well rounded	<0.5–2.0	Ag, Cu, Hg, Ti, V, Mn, Fe	Recrystallization, twinning, high-fineness segregation
Gaffney Find (lode)	149047	8	0.1–0.9 (0.7)	Irregular cemented, lumpy	Uneven, pitted	Slightly- and subrounded	2.5–4.0	Ag, Cu, Hg, Sb, V, Mn, Fe	Recrystallization, twinning, intergranular veinlet, high-fineness segregation
Gaffney Find (alluvium)	149071	2	1.3, 1.6	Well-rounded, originally lumpy or semi-idiomorphic	Even, with grooves and scratches	Well-rounded	<0.5	Ag, Cu, Hg, Ti, Fe	–
Low Hill (lode)	– ^(a)	–	0.07–1.0 (0.2)	Fine films of spongy gold	Spongy	Not rounded	<0.5	–	–
Cobra (lode)	149057	50	0.1–2.7 (0.3)	Irregular cemented, lumpy, and cellular	Uneven, spongy, cellular, platy	Angular, slightly rounded	9.2–19.0 (mean 10.7)	Ag, Cu, Hg, Zn, Sb, Pb, V, Mn, Fe, Co, Ni	High-fineness intergranular veinlets, partly recrystallized
McCarthys Patch (alluvium)	149074 (149062)	21	0.4–1.8	Rounded, originally semi-idiomorphic or cemented	Even, pitted	Well-rounded	5.6–7.8	Ag, Cu, Hg, Sb, Ti, Fe	Intergranular veinlets, irregular high-fineness rim

NOTES: Assay data from SEM-EDX analysis conducted by CSIRO, Kensington, Western Australia. Detection limit: 0.5 wt%

(a) Unnumbered sample provided for study by Mr. David Vaughan

Table 3. Laser Ablation-Inductively Coupled-Mass Spectrometry data for gold from Hibernian, Gaffney Find, Low Hill, Cobra, and McCarthys Patch

	Egerton - Hibernian - alluvial gold													
	149070A	149070B	149070C	149070D	149070E	149070F	149070G	149070H	149070I	149070J				
Sc	3 756	11 650	314	1 011	927	703	3 044	7 400	86	59	21 043	6 270	3 030	0
Ti	15 694	75 467	1 640	1 631	773	3 376	3 102	2 696	1 021	687	30 884	17 228	10 278	111
V	13 005	97 318	66	1 735	667	1 423	4 454	1 055	350	0	118 149	32 171	7 694	92
Cr	1 138	6 586	157	1 111	265	2 655	1 240	2	143	0	5 524	2 425	575	76
Mn	21 203	131 422	648	2 990	1 511	6 944	29 459	2 242	1 026	436	168 928	75 015	67 092	1 047
Fe	121 778	1 161 760	2 873	17 605	9 089	14 967	269 644	10 537	6 026	951	1 454 062	432 179	191 902	1 406
Co	783	3 538	0	24	20	270	159	270	0	2 187	7 300	2 593	1 388	0
Ni	1 661	5 407	167	0	308	1 462	1 423	0	29	167	6 637	2 094	1 090	0
Cu	631 748	176 148	87 695	583 757	422 188	1 097 579	871 805	544 678	291 320	15 810	236 401	179 739	268 844	80 228
Zn	2 752	8 115	106	50	187	5 903	9 532	186	112	71	22 100	6 380	3 619	109
Ga	3 308	12 465	300	602	566	752	1 227	1 126	177	315	43 125	5 274	2 748	260
Ge	78	2	0	39	35	41	65	62	0	78	177	93	44	0
As	322	2 308	0	0	10	41	4 939	45	18	54	1 705	461	37	26
Se	25	0	634	0	89	0	0	0	1	29	0	0	0	37
Rb	4 689	13 653	116	623	343	585	279	215	215	98	75 510	10 006	3 437	271
Sr	2 863	9 068	98	208	403	2 402	892	401	146	14	13 564	6 326	2 429	72
Y	561	3 027	0	103	103	4 951	289	41	41	0	7 290	1 449	630	35
Zr	1 540	19 327	227	170	125	435	16 005	182	1 966	1	46 192	10 339	3 227	0
Nb	399	2 057	313	226	0	94	0	12	0	0	990	593	430	0
Mo	3	0	0	49	78	67	72	0	43	37	83	27	8	27
Ru	0	8	29	0	15	0	0	27	32	0	35	0	32	0
Rh	78	24	53	48	39	141	99	92	14	18	0	24	0	0
Pd	2 512	61	96	3 271	16	16	45	1 155	1 152	70	75	109	12 905	123
Ag	39 712 116	10 374 784	7 124 533	27 622 494	17 844 398	42 285 448	46 405 060	19 064 518	55 608 276	2 680 565	38 880 884	33 311 298	58 603 552	8 608 076
Cd	108	163	79	151	0	223	130	167	243	90	69	52	143	84
In	66	68	51	0	38	10	0	40	0	0	82	0	21	47
Sn	617	1 519	902	516	301	407	257	567	451	266	1 129	1 191	313	273
Sb	10 815	267	4 606	114	29	205	127	22	0	34	237	159	105	235
Te	985	51	211	27	27	9	140	0	0	25	265	202	7	0
Ba	1 274	3 873	53	162	210	290	235	112	19	34	48 076	3 452	1 343	18
La	816	2 940	11	816	571	1 592	316	11	66	5	2 960	1 108	1 108	46
Ce	616	3 759	73	654	1 379	230	327	169	116	0	4 931	1 427	2 015	0
Pr	145	729	1	12	132	58	122	6	20	0	1 102	340	324	18
Nd	66	468	21	7	133	86	64	1	6	9	787	447	494	21
Sm	16	179	0	11	40	18	73	12	0	0	336	53	49	0
Eu	0	20	1	0	895	0	62	44	0	0	225	48	5	28
Gd	30	165	0	16	6	0	91	1	0	0	245	43	7	31
Tb	79	101	0	26	46	0	27	0	28	0	149	59	77	0
Dy	24	70	14	12	30	22	172	35	0	0	413	64	71	22
Ho	48	85	43	16	5	38	129	18	0	9	321	79	0	22
Er	37	115	11	0	2	4	395	25	10	0	421	0	22	0
Tm	0	22	28	0	0	0	85	17	0	4	228	60	15	4
Yb	6	170	0	0	37	1	179	50	0	0	621	90	34	0
Lu	0	94	7	13	9	0	30	27	213	0	289	73	28	7
Hf	164	218	14	0	16	1	282	20	7	8	852	202	47	0
Ta	13	90	428	0	10	0	58	0	0	0	49	18	14	7
W	14	206	0	19	64	3	55	0	8	18	113	10	54	0
Re	0	13	0	0	0	0	7	0	0	0	28	51	6	16
Os	7	28	0	0	0	0	0	13	15	0	0	0	10	12
Ir	11	23	0	3	12	0	0	15	0	39	0	0	14	3
Pt	12	11	0	2	42	0	382	42	0	15	25	0	13	13
Hg	852 965	230 832	66 882	943 342	459 644	471 495	227 009	598 690	6 111 938	1 736	456 117	369 729	1 226 309	151 148
Tl	137	122	132	28	4	2	0	0	21	8	513	100	24	0
Pb	862	66 316	1 374 756	132	59	1 768	16 619	15	81	19	2 997	1 019	1 218	31
Bi	348	5 441	95 929	18	90	7	348	44	440	6	486	385	165	483
Th	299	2 612	26	22	8	8	564	51	0	30	5 081	803	871	1
U	59	326	9	0	28	390	0	0	0	31	981	129	155	0

Table 3. (continued)

	Egerton - Hibernian - alluvial gold					Egerton - Gaffney Find - lode gold						
	14907002	1490700G	1490700H	1490700I	1490700L	1490700K	Average	149047D	149047D2	149047E	149047C	149047A
Sc	0	6835	14907002	942	1746	2209	3337	950	942	2116	4142	3889
Ti	0	53415	9799	5409	8362	3915	11811	313	418	600	1931	1531
V	0	38861	5165	2337	6479	2120	15213	2401	7656	8367	9201	9706
Cr	0	2835	780	443	592	486	1070	6199	206	5189	440	408
Mn	0	53507	5659	5751	33874	4911	27978	15039	5394	13079	146204	32208
Fe	0	38155	36849	39540	87795	36074	194518	38314	8087	58619	133810	79653
Co	0	1639	374	81	844	197	977	545	299	369	1757	2947
Ni	0	2612	720	87	726	138	1076	145	104	589	594	658
Cu	27106	61121	913	101591	296715	264461	283636	422725	532265	880966	955222	696344
Zn	0	4757	1461	440	1455	788	3105	0	914	524	2438	1612
Ga	0	7358	2810	1395	1985	896	3995	446	135	770	2336	1513
Ge	33	98	0	0	0	0	45	77	0	0	0	0
As	0	880	89	0	92	10	502	302	46	90	208	204
Se	11	0	0	0	107	37	45	0	43	0	43	0
Rb	0	11664	2127	835	3127	716	5861	454	169	279	955	243
Sr	0	5470	1806	612	1285	1522	2260	620	144	512	1314	661
Y	0	1899	319	284	640	12953	1573	123	26	80	63	20
Zr	0	11111	1180	1558	1044	98709	9710	280	5	242	4289	88
Nb	0	1744	169	98	296	0	345	12	38	45	56	174
Mo	0	1639	112	40	114	176	52	0	0	0	91	105
Ru	0	0	6	0	25	63	15	54	33	17	0	60
Rh	18	21	51	32	22	55	38	101	38	105	108	18
Pd	141	693	1464	118	2526	53	1217	551	468	543	501	422
Ag	4286811	4666315	4650492	1883332	1474155	33180628	22229878	50076600	50761796	46564980	61713856	39447052
Cd	80	109	0	202	11	123	109	156	0	179	76	0
In	0	0	44	0	0	38	24	0	0	349	74	49
Sn	0	1015	315	430	466	422	553	420	652	375	264	397
Sb	0	269	125	330	114	97	814	1894	1476	1268	1943	976
Te	0	0	8	74	51	411	113	18	86	2776	162	218
Ba	0	5553	3232	426	1363	518	3196	150	69	447	170	431
La	0	3169	1520	157	637	46	210	46	28	72	95	102
Ce	0	4157	2880	171	714	381	1092	46	23	111	306	209
Pr	4	916	293	106	148	64	208	9	0	28	269	29
Nd	0	579	258	0	92	10	161	0	0	3	33	42
Sm	0	199	42	0	0	0	49	36	10	9	35	20
Eu	0	43	1	7	51	55	69	27	8	0	2	7
Gd	0	153	4	73	18	94	44	21	0	8	0	0
Tb	0	73	72	34	29	231	50	10	0	0	31	0
Dy	0	167	33	12	25	478	77	20	28	7	5	0
Ho	0	120	38	29	22	706	79	0	0	0	29	0
Er	0	101	0	37	40	1079	108	23	177	0	0	0
Tm	0	64	26	3	0	547	52	34	0	27	0	9
Yb	0	170	0	46	22	1321	125	0	0	6	0	0
Lu	0	55	7	33	44	650	72	48	47	0	20	0
Hf	0	246	0	37	40	2015	191	0	16	25	0	0
Ta	0	179	56	0	11	22	46	0	0	26	0	0
W	0	153	46	0	92	24	40	65	29	407	534	223
Re	1	0	1	0	7	0	6	0	0	0	0	1
Os	0	10	0	0	14	11	6	0	24	0	2	0
Ir	19	29	1	12	0	10	11	0	0	0	21	0
Pt	31	0	20	0	0	41	30	11	0	0	0	17
Hg	46698	41072	3894	204714	527550	493222	363061	54345	42954	26103	44829	17705
Tl	0	80	42	0	11	0	57	3	0	0	21	0
Pb	0	5583	571	450	170	258	66953	170	629	1201	1723	486
Bi	0	1532	41	1478	70	317	4895	1591	586	17643	1357	1317
Th	0	2623	363	409	240	1022	688	141	10	16	32	30
U	0	425	43	73	44	685	154	45	19	71	169	229

Table 3. (continued)

	Egerton - Gaffney Find - lode gold				Egerton - Gaffney Find - alluvial gold				Bancroft - Coburn - lode gold				
	I49047A2	I49047B	I49047F	I49047G	I49047H	I49077A	I49077B	I49077A1	Average	I49057A	I49057B	I49057C	I49057C2
Sc	136	1136	2329	8473	19024	337	1052	53	481	4377	2875	3212	5709
Ti	35	631	1550	1972	2166	1029	1046	1190	1088	737678	776	234	4944
V	1108	8967	16618	28131	21669	203	400	623	409	67167	12351	7713	18216
Cr	118	1767	1328	12139	847	211	0	0	70	7030	101616	484	13820
Mn	4623	9470	109560	44525	17871	2165	457	273	665	1236059	855882	1019038	1576451
Fe	10241	43181	85933	187861	277495	4728	4765	6940	5478	120230	401638	140857	291676
Co	65	607	678	1171	916	107	84	113	101	49977	60047	11259	30608
Ni	75	371	835	513	1650	25	25	166	64	2410	5689	1602	2686
Cu	920922	755967	296159	873162	142224	844	31975	266724	99848	151141	232516	149618	183328
Zn	0	370	783	1813	13985	0	230	180	137	6863	14563	3547	14808
Ga	203	2054	1193	2535	15687	311	352	196	286	2399	1338	743	3199
Ge	0	4	58	113	138	51	16	29	32	0	97	0	23
As	0	243	63	183	5519	81	191	33	102	568	548	362	363
Se	0	0	0	127	136	18	0	29	16	0	0	0	0
Rb	0	50	387	415	18446	4918	143	80	1714	748	1133	3857	1175
Sr	280	116	1256	1922	17695	107	64	196	122	14994	6343	4669	22706
Y	22	48	68	15559	275	77	56	33	55	6185	615	286	3243
Zr	0	40	211	546	17884	259	226	376	287	22675	1599	1639	6672
Nb	75	0	29	125	0	0	150	60	70	31025	17	121	221
Mo	103	0	31	210	127	166	11	33	70	369	406	49	398
Ru	0	24	0	14	47	11	0	0	4	33	39	23	18
Rh	120	135	40	0	16	7	6	33	15	23	30	2	60
Pd	499	691	989	1179	613	22	153	116	97	680	407	445	542
Ag	49304584	44695200	161806528	46796380	129691	1196976	2134691	15489566	6273744	177240976	233428624	212295856	236001952
Cd	13	52	109	0	0	62	0	39	34	165	219	299	809
In	39	0	8	67	108	0	0	43	14	46	0	28	65
Sn	405	343	229	469	1097	144	300	465	196	1422	633	830	2647
Sb	1403	1467	3874	4276	2417	44	124	739	302	2981	34248	9491	9503
Te	105	2038	103	0	161	0	567	0	0	174	4	19	14
Ba	152	47	391	1257	10340	259	144	0	134	1771	457	530	4157
La	0	68	82	139	6041	59	172	0	77	252	127	276	428
Ce	0	36	93	243	586	148	188	0	112	750	724	175	1197
Pr	7	3	22	81	350	11	0	0	4	140	26	79	223
Nd	0	1	1	135	97	0	24	0	8	141	123	51	226
Sm	0	0	0	180	44	0	0	0	0	40	28	41	78
Eu	3	4	9	213	0	0	0	0	13	91	16	46	79
Gd	7	0	20	346	0	0	14	0	12	173	52	63	76
Tb	2	73	480	435	61	0	18	0	6	140	0	0	58
Dy	13	0	18	811	16	0	0	0	0	215	17	9	110
Ho	0	0	21	732	2	18	0	0	6	217	0	0	79
Er	0	34	16	617	49	11	25	0	12	172	55	0	58
Tm	4	21	0	1801	19	0	0	0	4	75	0	0	72
Lu	11	0	13	2249	438	7	91	0	33	179	27	11	72
Hf	2	27	0	2322	0	0	14	0	5	100	0	0	36
Ta	0	0	0	11	161	18	0	0	6	351	6	14	18
W	17	69	227	444	749	14	0	0	2	2654	0	0	20
Re	16	25	8	0	0	18	0	16	5	24975	169	93	283
Os	0	0	0	0	33	0	16	0	11	8	14	47	17
Ir	0	11	0	0	0	25	2	0	9	0	9	1	13
Pt	12	5	3	17	602	18	0	3	7	0	10	0	13
Hg	24240	20414	74144	26298	708	707	1567	9928	4067	299076	384728	472660	533001
Tl	0	0	2	95	72	7	0	0	2	16	27	0	31
Pb	3282	399	2868	203	4528	62	208	0	90	8015	9238	14121	54551
Bi	2088	14052	2114	276	219	0	87	313	133	752	283	511	770
Th	31	11	56	36	127	25	36	0	20	1101	223	15	192
U	0	100	138	260	713	29	13	0	14	635	277	84	421

Table 3. (continued)

	149057D	149057E	149057F	149057G	149057I	149057H	149057J	149057K	149057L	149057M	149057N	149057O	149057P	149057Q
Sc	353	2 476	3 110	610	2 226	359	944	451	0	2 552	1 372	197	1 953	898
Ti	351	403	37 949	373	400	5	2 210	208	293	494	479	148	784	99
V	2 383	8 084	21 656	3 655	6 022	346	6 681	458	2 027	5 562	8 158	14 670	6 921	13 189
Cr	213	16 829	16 099	873	590	116	159	311	101	5 486	292	486	45	0
Mn	156 695	380 435	513 344	1 203 750	406 211	145 942	400 934	47 528	455 987	1 347 746	2 569 348	1 109 045	303 082	96 093
Fe	44 894	152 892	221 658	209 804	122 253	6 295	239 474	16 624	19 233	256 043	607 129	6 929	809 482	391 490
Co	10 366	6 050	18 784	8 699	30 668	3 591	5 210	740	6 252	5 488	7 773	26 912	6 066	6 558
Ni	2 252	1 446	2 043	1 331	1 169	77	920	484	378	2 466	5 246	929	2 433	2 355
Cu	208 581	125 549	173 560	103 074	133 035	20 876	28 518	26 069	80 800	160 725	61 032	101 573	57 399	70 210
Zn	1 757	4 426	6 937	7 464	4 030	1 153	7 128	499	1 924	31 516	20 102	1 103	22 654	26 877
Ga	1 172	1 484	2 613	5 912	887	178	884	178	868	1 549	339	2 522	788	570
Ge	0	15	67	0	0	147	24	40	56	0	87	82	0	0
As	161	341	257	297	1 010	32	458	71	32	302	334	1	547	1 565
Se	13	0	0	0	21	22	0	50	0	256	0	0	265	0
Rb	188	2 765	2 319	527	222	202	79	0	59	514	107	329	238	0
Sr	2 059	4 515	9 990	10 461	12 829	1 506	2 568	498	18 216	9 426	1 717	13 096	3 839	873
Y	466	497	1 506	419	365	32	294	14	122	537	456	137	1 009	374
Zr	156	1 446	5 093	987	5 601	294	788	194	297	2 248	2 039	128	7 478	1 688
Nb	0	0	850	13	0	0	51	143	15	161	258	173	10	202
Mo	0	15	219	219	203	93	156	0	0	80	177	26	309	265
Ru	4	8	30	0	0	0	0	0	0	16	11	34	0	34
Rh	75	44	36	23	39	13	0	0	54	0	37	40	0	0
Pd	408	783	382	806	731	2 695	2 461	2 253	423	1 512	2 531	750	2 333	1 222
Ag	163 987 760	209 207 616	186 281 680	216 519 408	195 149 120	342 062 688	401 669 696	398 826 464	164 908 416	192 154 512	338 106 304	219 350 112	379 432 672	329 268 192
Cd	149	128	204	57	28	71	0	154	149	249	215	144	181	37
In	0	28	12	569	74	13	24	24	102	75	37	35	27	2
Sn	575	1 095	563	3 557	4 280	705	604	499	434	418	1 155	6 439	528	457
Sb	3 407	2 954	29 690	3 436	3 904	7 876	30 064	25 367	4 558	2 812	6 768	2 765	29 402	4 398
Te	18	31	31	329	107	17	46	12	191	32	758	0	112	51
Ba	344	982	1 637	4 002	704	64	536	57	766	816	482	2 323	352	137
La	26	75	211	188	118	27	29	16	80	141	73	92	97	103
Ce	91	158	580	596	159	54	133	36	162	204	805	480	230	102
Pr	27	80	139	48	101	1	0	32	23	34	3	32	68	3
Nd	0	41	85	28	18	119	0	11	45	61	12	56	57	0
Sm	6	0	28	27	12	8	7	0	61	2	2	6	54	25
Eu	0	252	37	35	56	12	0	0	30	23	27	22	24	65
Gd	26	13	62	52	0	0	20	0	11	23	0	16	60	17
Tb	0	60	4	0	46	39	63	0	71	0	56	0	72	20
Dy	0	0	65	12	7	11	36	13	62	30	0	38	41	2
Ho	0	54	62	16	0	0	30	43	43	59	0	11	85	24
Er	4	28	65	4	0	11	5	9	8	35	15	4	30	37
Tm	0	0	34	16	7	0	12	7	5	30	13	0	36	0
Yb	4	23	62	14	29	30	0	0	70	24	24	0	27	34
Lu	0	30	5	24	23	25	0	0	0	0	4	0	19	37
Hf	2 689	28	48	18	40	65	24	2	11	47	11	0	39	0
Ta	0	0	89	0	0	0	22	0	11	15	0	22	0	0
W	31	45	4 585	50	121	0	34	0	23	0	111	122	0	45
Re	0	0	0	65	0	19	0	0	6	12	17	0	19	0
Os	27	0	0	0	19	0	7	0	6	0	20	0	2	0
Ir	0	0	11	0	6	16	0	0	15	0	26	0	4	0
Pt	129	0	0	7	31	0	37	0	0	0	26	0	5	0
Hg	372 808	435 980	342 695	1 050 397	419 792	798 763	399 871	368 837	361 121	427 930	986 695	463 053	354 631	1 135 555
Tl	13	25	5	0	41	4	0	0	16	7	56	0	29	226
Pb	3 706	10 836	9 870	18 120	98 998	288	8 421	949	11 671	38 804	16 460	64 591	37 073	17 232
Bi	79	116	145	684	1 302	277	322	216	105	295	3 035	86	719	2 040
Th	2	45	116	34	35	0	30	0	5	60	50	36	86	10
U	48	60	267	83	235	13	18	0	61	85	217	308	47	259

Table 3. (continued)

	Bengemall - Cobna - Lode gold					Bengemall - McCarthys Patch - alluvial gold							
	149057R	149057S	149057T	149057U	Average	149074H	149074G2	149074J	149074K	149074L	149074C	149074D	149074A
Sc	653	1 375	5 266	0	1 862	1 009	1 676	860	820	1 224	3 264	4 855	1 203
Ti	81	462	7 876	451	3 624	4 630	6 298	4 953	536	2 273	11 806	5 732	2 707
V	3 450	3 008	15 850	3 241	10 491	1 618	885	1 382	294	872	6 338	5 916	905
Cr	2 615	241	7 675	490	7 675	322	0	449	41	0	0	366	0
Mn	46 365	1 797 134	1 467 754	269 886	791 123	1 435	1 834	759	76	1 155	4 122	7 387	1 398
Fe	75 804	74 179	504 898	63 026	216 205	12 470	6 965	3 451	5 800	6 809	27 120	27 601	6 004
Co	1 535	19 591	23 323	4 931	15 656	103	0	198	185	297	144	673	386
Ni	447	2 059	4 911	718	2 002	0	18	344	113	15	342	138	48
Cu	131 140	95 225	86 041	92 113	112 369	74 094	7 328	74 088	47 730	60 402	78 578	83 304	84 972
Zn	4 347	2 537	18 024	1 268	9 251	0	344	144	300	0	170	463	555
Ga	888	865	2 665	609	1 485	649	540	321	449	691	1 788	844	662
Ge	0	0	152	0	36	82	0	0	109	97	0	64	67
As	69	151	579	0	368	0	7	0	119	13	0	137	86
Se	116	14	0	9	35	0	0	33	0	110	0	54	7
Rb	84	104	1 349	502	750	471	288	472	38	319	516	1 011	188
Sr	2 340	9 667	16 944	2 528	7 808	200	92	145	42	67	900	2 641	114
Y	137	396	24 824	124	1 911	61	81	127	10	0	107	90	0
Zr	718	925	92 555	367	7 072	230	137	2 522	31	172	954	209	2 899
Nb	0	15	146	0	1 519	5	37	38	89	284	122	463	122
Mo	172	129	220	171	167	136	29	0	74	140	185	355	103
Ru	0	0	9	3	12	0	0	0	0	17	52	0	1
Rh	0	0	62	26	26	0	0	51	14	30	34	0	16
Pd	361	391	1 308	380	1 082	6	11	69	42	114	66	33	6
Ag	187 212 480	148 723 616	182 414 944	175 879 232	240 460 105	145 230 016	40 547 748	90 749 672	80 512 024	73 345 920	80 910 904	96 930 464	47 556 936
Cd	123	141	68	41	165	66	11	61	57	31	11	163	95
In	1	0	77	154	63	31	0	54	6	61	43	48	120
Sn	800	531	804	254	1 329	543	511	711	485	493	589	663	341
Sb	18 087	12 129	1 950	3 791	11 345	31 946	4 108	22 313	58 802	3 327	1 907	5 438	4 044
Te	0	0	150	0	94	87	0	8	76	4	0	0	0
Ba	49	599	2 780	764	1 105	173	66	0	90	6	600	227	33
La	90	0	269	105	128	5	0	0	38	0	138	45	0
Ce	219	194	7 666	459	690	30	11	0	38	58	500	259	59
Pr	39	26	213	6	61	19	29	600	19	14	0	40	7
Nd	9	0	265	17	62	31	0	0	9	0	26	14	9
Sm	12	12	320	1	34	11	829	18	0	0	0	26	2
Eu	13	6	488	0	60	36	70	7	33	32	0	22	0
Gd	90	25	814	33	74	19	0	0	4	6	22	9	16
Tb	12	15	1 152	3	84	15	0	0	19	104	0	69	24
Dy	0	0	814	23	69	4	11	0	9	12	0	25	0
Ho	8	8	611	15	54	0	0	0	0	14	6	13	5
Tm	23	33	390	53	36	22	7	20	0	16	4	15	14
Yb	4	403	584	2	74	20	0	0	0	0	34	15	14
Lu	0	92	284	0	31	15	0	0	0	0	0	0	59
Hf	26	25	712	1	187	10	18	0	0	26	14	17	36
Ta	5	0	132	2	132	1	11	0	0	35	41	16	0
W	22	44	117	0	1403	0	0	0	0	7	16	0	14
Re	0	0	4	0	10	0	14	0	0	0	20	0	0
Os	9	22	0	0	7	36	18	11	0	18	0	0	0
Ir	10	0	0	16	6	30	3	0	0	25	34	0	0
Pt	0	5	0	2	12	30	3	16	19	28	0	0	0
Hg	381 346	397 492	1 004 633	402 149	536 964	2 042 733	140 102	2 213 298	559 002	208 912	288 289	1 049 789	58 429
Tl	33	0	10	0	25	0	62	0	0	44	0	122	18
Pb	5 972	8 625	24 612	6 629	21 308	0	196	0	33	56	49	121	123
Bi	59	178	1 036	107	596	0	74	0	33	67	41	18	32
Th	18	69	677	103	132	0	0	0	47	50	65	46	13
U	222	61	735	17	189	0	0	0	14	7	0	33	5

Table 3. (continued)

	Bengeruall - McCarthys Patch - alluvial gold											Average
	149074M	149074N	149074O	149074P	149074F	149074Q	149074R	149074E	149074S	149074B2	149074T	
Sc	1 328	803	358	637	907	457	617	687	24 292	0	478	470
Ti	6 346	1 196	566	8 867	1 553	873	1 238	3 036	291 792	1 168	4 623	4 270
V	3 399	405	124	5 349	176	373	577	553	274 862	521	3 123	2 624
Cr	352	117	183	133	0	0	166	0	15 899	0	237	161
Mn	3 123	934	1 511	1 552	948	219	642	584	137 928	109	3 117	5 099
Fe	18 689	1 912	1 080	10 960	2 932	1 750	3 941	2 401	1 653 924	3 658	18 713	23 614
Co	146	183	0	14	30	90	75	36	4 818	81	166	191
Ni	753	82	87	0	121	791	116	347	9 794	367	166	153
Cu	17 121	4 609	79 481	90 506	6 625	21 964	76 144	42 131	20 009	25 149	58 043	158 235
Zn	209	0	79	46	0	20	0	5	11 532	0	114	562
Ga	564	761	458	880	438	115	183	309	18 556	203	1 044	1 432
Ge	0	3	120	0	2	0	63	50	346	189	192	87
As	0	0	0	32	45	0	0	28	2 136	94	25	0
Se	0	0	0	0	132	315	83	0	0	92	0	20
Rb	1 157	265	295	276	135	138	111	131	13 224	73	144	592
Sr	551	20	33	196	88	75	83	293	11 114	77	533	165
Y	97	0	4	43	25	11	43	4	15 791	0	114	83
Zr	293	22	0	2 669	57	0	102	52	34 846	47	355	217
Nb	282	0	20	105	73	119	0	275	6 028	147	118	94
Mo	313	55	104	0	51	58	0	94	226	68	22	0
Ru	34	16	0	0	45	0	44	0	0	4	11	0
Rh	0	14	0	37	5	42	100	0	0	0	0	0
Pd	37	0	58	13	11	26	0	45	33	0	0	0
Ag	149 730 000	16 830 640	93 587 080	143 326 896	18 434 646	23 083 186	59 846 836	106 100 728	10 608 295	30 361 958	76 255 288	124 816 160
Cd	15	0	0	62	83	31	119	64	0	60	148	24
In	9	0	0	0	49	65	138	0	76	0	31	174
Sn	540	660	571	665	430	418	747	559	2 507	397	685	444
Sb	42 960	995	12 043	26 226	1 122	6 986	38 129	1 972	12 420	6 513	5 060	26 410
Te	3	38	37	0	3	35	0	0	0	0	22	0
Ba	306	65	29	34	78	46	0	33	5 971	69	681	56
La	59	157	0	63	10	0	0	6	10 140	65	85	36
Ce	220	72	8	220	36	0	0	27	12 496	64	55	128
Pr	22	9	4	0	10	0	0	29	2 440	0	29	10
Nd	3	0	33	28	0	0	0	0	1 536	2	11	15
Eu	33	9	0	4	0	43	0	22	399	0	7	0
Gd	6	23	8	0	12	0	0	6	266	0	11	11
Tb	0	61	54	0	0	22	2	11	509	7	11	0
Dy	2	0	12	9	0	0	0	45	396	17	0	0
Ho	20	28	8	0	5	0	19	13	760	14	3	49
Er	23	3	49	0	0	1	0	13	629	0	0	0
Tm	9	6	0	0	0	20	0	4	476	22	25	0
Yb	0	0	0	0	0	0	19	28	0	0	0	0
Lu	0	0	0	9	0	0	0	0	836	5	25	0
Hf	49	1	8	29	0	21	0	0	249	0	0	0
Ta	19	8	0	13	2	0	8	0	213	0	14	39
Ta	19	8	0	13	2	0	8	0	863	0	14	39
W	23	3	287	0	27	0	2	0	590	34	33	14
Re	26	3	8	6	0	3	2	0	313	0	25	0
Os	6	0	12	13	21	0	0	13	0	0	29	4
Ir	0	27	0	0	41	0	0	52	43	0	0	0
Pt	14	2	0	0	30	0	0	0	0	0	0	0
Hg	887 003	126 018	394 301	2 159 785	186 654	102 271	106 992	653 675	67 069	162 596	967 051	2 032 101
Tl	13	23	37	10	0	10	149	26	106	46	22	56
Pb	130	26	0	21	68	55	0	49	10 327	0	33	70
Bi	109	6	8	0	45	0	213	24	916	0	14	0
Th	26	10	0	0	20	26	14	14	5 451	34	66	21
U	10	7	8	88	0	0	0	11	466	0	0	27

Table 4. Laser Ablation-Inductively Coupled Plasma-Mass Spectroscopy

NST 610													Average
Sc	738 357	854 162	878 210	983 372	990 330	956 634	732 382	728 041	812 220	603 287	602 427	620 578	791 667
Ti	38 137	45 098	47 094	51 663	53 501	50 153	39 330	39 079	42 478	31 503	32 113	33 625	41 981
V	656 669	758 103	793 070	884 219	927 963	878 255	679 989	665 157	721 980	525 557	556 565	569 499	718 086
Cr	60 879	66 562	72 888	89 453	88 860	81 043	55 687	55 774	59 313	45 308	47 426	50 296	64 457
Mn	804 934	897 256	964 566	1 246 034	1 171 755	1 121 095	754 532	771 168	826 383	606 477	633 243	636 203	869 471
Fe	23 461	26 662	26 782	32 572	30 679	30 955	22 593	21 998	22 541	17 231	16 857	18 037	24 197
Co	554 361	637 576	690 436	875 304	813 626	797 281	559 980	557 252	587 237	443 044	427 058	521 884	622 087
Ni	130 767	146 078	153 184	196 066	183 764	183 962	122 149	121 952	132 720	99 916	98 527	110 145	139 936
Cu	194 794	197 270	285 724	344 370	250 878	282 073	221 844	211 362	186 606	133 270	131 800	220 571	221 714
Zn	92 286	110 595	119 940	90 611	103 528	112 526	103 345	103 041	106 904	84 073	91 587	96 696	101 261
Ga	524 657	585 199	632 190	856 917	790 904	813 044	501 997	506 870	545 468	424 649	450 660	513 956	595 543
Ge	50 847	56 222	59 368	75 766	71 866	70 636	48 409	48 577	53 256	40 776	45 259	48 426	55 784
As	80 773	95 662	104 494	77 355	82 964	89 468	99 797	100 158	107 933	74 850	83 892	87 059	90 367
Se	6 534	7 314	7 664	5 982	6 330	6 701	7 610	7 671	8 032	5 610	6 448	7 039	6 911
Rb	478 090	503 353	521 206	685 217	640 446	679 063	466 352	473 032	497 107	386 438	417 381	522 931	522 551
Sr	751 626	829 601	832 859	1 072 233	1 003 109	1 027 529	753 997	763 881	818 125	575 068	638 130	763 078	819 103
Y	598 569	685 411	713 363	820 222	814 951	854 466	623 211	642 335	680 768	498 729	559 484	625 129	676 387
Zr	268 085	295 194	309 739	336 933	341 407	346 620	276 853	280 617	304 212	227 098	247 600	273 526	292 324
Nb	490 574	541 652	575 432	630 349	653 059	670 308	500 460	508 818	543 281	420 004	449 032	518 849	541 818
Mo	81 455	89 454	94 688	106 778	108 353	108 156	82 380	86 053	88 855	67 835	78 427	85 964	89 867
Ru	33	0	0	0	49	57	22	1	42	0	0	20	19
Rh	1 794	1 949	2 180	2 779	2 598	2 552	1 688	1 819	1 776	1 414	1 553	1 720	1 985
Pd	2 218	2 685	2 565	3 188	3 217	2 809	2 441	2 313	2 377	1 759	2 017	2 352	2 495
Ag	158 620	180 112	187 295	241 824	232 118	226 635	166 390	167 438	168 749	134 355	149 871	167 960	181 781
Cd	28 072	31 711	33 868	31 954	34 420	33 824	29 833	28 803	30 214	24 990	26 673	27 682	30 170
In	678 237	803 341	851 437	1 153 102	1 082 464	1 033 814	753 467	744 670	773 707	613 271	682 238	790 386	830 011
Sn	253 514	292 217	311 928	398 559	385 028	352 943	273 704	276 231	283 486	232 984	256 772	278 837	299 684
Sb	243 850	276 737	303 990	284 162	295 456	295 213	280 024	276 232	291 256	230 465	259 853	269 457	275 558
Te	43 663	52 171	57 433	44 832	50 832	52 116	56 292	54 798	58 710	47 768	52 955	58 453	52 502
Ba	62 674	72 069	79 932	92 494	89 635	87 487	72 189	72 406	77 313	61 700	65 823	74 667	75 699
La	437 611	508 940	540 055	520 104	561 713	576 035	524 349	535 517	569 711	445 351	505 320	550 322	522 919
Ce	479 237	553 961	597 060	587 959	640 487	632 959	573 763	591 513	642 481	494 632	549 464	624 581	580 675
Pr	658 469	786 195	819 388	897 684	950 164	937 285	772 304	794 649	864 378	625 844	732 685	781 324	801 697
Nd	109 647	126 082	132 184	150 407	150 895	151 926	123 662	129 702	137 934	103 240	117 557	117 618	129 238
Sm	181 334	206 988	216 178	266 437	262 461	255 276	204 887	215 091	228 228	173 574	192 556	194 938	216 496
Eu	379 909	442 151	455 708	571 259	565 196	545 492	431 101	451 936	479 461	355 440	399 712	421 988	458 279
Gd	147 491	162 534	170 924	216 742	211 528	208 056	161 750	169 447	178 724	133 689	147 364	162 000	172 521
Tb	635 630	734 426	793 362	952 859	962 612	958 249	733 651	759 073	819 850	575 473	646 833	730 659	775 223
Dy	158 561	175 740	185 540	229 543	230 764	222 832	178 383	183 503	196 775	141 788	156 093	178 939	186 538
Ho	620 058	715 755	769 059	972 398	943 386	954 832	733 499	741 838	795 504	571 387	601 602	737 688	763 084
Er	209 430	230 490	248 981	305 098	297 941	295 615	238 347	241 851	258 264	195 152	200 787	236 586	246 545
Tm	670 898	733 554	803 380	1 008 068	1 006 342	983 344	761 821	776 156	827 056	602 939	613 007	771 835	796 533
Yb	226 400	250 528	261 702	349 790	333 969	321 434	254 181	257 696	272 217	207 371	213 656	252 834	266 815
Lu	614 424	689 924	721 188	952 477	918 508	944 911	699 742	722 323	765 586	587 176	616 214	728 421	746 741
Hf	158 020	177 518	181 512	215 207	217 278	229 211	180 893	184 867	195 361	155 746	161 249	184 505	186 781
Ta	475 411	538 657	557 071	663 365	665 831	725 408	549 023	555 215	592 967	470 658	484 807	551 307	569 143
W	114 863	127 466	132 517	157 744	157 115	167 888	126 735	127 399	141 617	107 627	108 615	133 162	133 562
Re	26 248	28 249	29 607	38 122	36 712	40 801	27 956	28 967	31 739	25 875	25 945	30 895	30 926
Os	5	4	16	12	19	0	23	0	11	2	25	0	10
Ir	102	122	127	152	145	128	98	109	86	98	72	76	110
Pt	761	897	954	1 034	1 036	1 119	888	802	946	711	749	887	899
Hg	1 026	1 387	1 348	858	402	762	967	752	908	50	165	484	759
Tl	52 021	58 790	60 445	85 959	83 614	78 428	56 478	58 516	61 192	46 660	53 973	60 489	63 047
Pb	251 817	288 473	303 447	416 511	411 607	390 950	286 281	288 485	314 690	228 209	264 506	294 689	311 639
Bi	427 576	483 134	506 799	694 744	700 038	641 721	463 765	473 263	525 516	378 566	437 957	470 527	516 967
Th	347 585	397 146	416 167	463 896	502 979	490 690	416 131	436 106	473 046	363 495	406 301	431 952	428 791
U	439 697	494 205	517 750	653 152	715 841	636 675	515 968	521 047	581 600	447 318	483 803	543 611	545 889

(LA-ICP-MS) data for reference samples Glass NIST 610, and Gold AUSTD1

		AUSTD1										
SD	Covariance									Average	SD	Covariance
143 408	18	0	31	431	933	1 608	563	594	607	102		
7 607	18	137	61	46	2 994	7 326	49	1 769	2 963	167		
134 097	19	137	66	923	1 306	528	290	542	486	90		
15 432	234	120	0	17	355	628	0	187	255	137		
216 288	249	3 506	4 295	3 202	13 454	7 145	5 832	6 239	3 834	61		
5 407	22	13 381	14 441	15 263	21 359	21 875	19 102	17 570	3 685	21		
144 727	23	729	2 039	780	27 164	37 519	3 037	11 878	16 208	136		
33 307	24	1 412	1 290	1 303	3 359	3 799	1 750	2 152	1 126	52		
61 943	28	13 771 224	13 904 637	13 522 984	17 611 382	19 581 188	18 306 540	16 116 326	2 689 014	17		
10 494	10	6 984	6 454	7 025	25 384	32 306	10 087	14 707	11 241	76		
146 547	25	66	267	163	2 320	582	254	609	856	141		
11 357	20	25	32	82	23	8	91	44	34	79		
11 002	12	97	0	53	97	52	205	84	69	83		
761	11	83	0	352	155	0	0	98	139	141		
96 788	19	331	135	624	4 233	1 582	271	1 196	1 577	132		
150 442	18	141	61	153	89 282	1 660	282	15 263	36 267	238		
109 115	16	0	0	13	78	49	194	56	74	134		
37 383	13	1 083	525	448	21 836	11 634	1 529	6 176	8 801	143		
78 193	14	0	3	0	329	41	52	71	128	181		
12 647	14	0	103	194	505	842	66	285	325	114		
22	117	31	0	0	57	9	0	16	23	144		
442	22	1 720	1 843	1 525	2 775	2 276	2 355	2 082	467	22		
433	17	3 394	3 146	3 711	4 371	4 847	3 871	3 890	629	16		
34 101	19	30 963 962	30 640 022	30 303 520	39 838 668	39 888 808	35 283 024	34 486 334	4 542 380	13		
3 049	10	0	54	134	185	190	122	114	75	65		
170 709	21	35	79	104	748	749	61	296	351	119		
52 610	18	220	301	244	2 462	1 384	415	838	910	109		
21 858	8	920	1 096	1 016	3 947	5 689	988	2 276	2 045	90		
5 050	10	20	114	70	714	553	90	260	295	113		
10 164	13	0	5	215	674	417	22	222	275	124		
44239	8	0	50	0	137	60	7	42	53	126		
53 874	9	1 017	219	132	5 387	3 038	501	1 716	2 095	122		
100 748	13	33	0	0	155	10	1	33	61	184		
16 205	13	0	0	8	9	0	24	7	9	137		
31 031	14	0	0	29	26	34	118	35	43	126		
70 557	15	41	0	0	12	24	0	13	17	131		
26 772	16	0	7	5	31	17	10	12	11	94		
129 333	17	18	0	21	25	0	0	11	12	112		
28 905	15	6	0	0	12	10	10	6	5	83		
135 401	18	6	15	0	30	111	0	27	43	158		
37 148	15	8	0	43	14	0	28	16	17	110		
140 708	18	6	0	17	188	2	0	36	75	211		
45 855	17	0	33	8	4	33	6	14	15	107		
127 381	17	16	14	0	29	0	0	10	12	121		
23 763	13	20	0	27	271	114	38	78	102	130		
80 228	14	4	16	20	12	12	0	11	7	70		
19 424	15	20	9	7	16	0	12	11	7	66		
5 020	16	0	0	3	3	11	0	3	4	150		
9	95	0	0	13	12	0	0	4	6	155		
26	23	10	0	38	10	55	32	24	21	87		
127	14	1 302	1 402	1 437	1 538	1 778	1 476	1 489	162	11		
421	55	2 547	1 876	1 951	16 895	14 168	11 490	8 155	6 827	84		
12 633	20	2	0	26	2	10	29	12	13	112		
61 881	20	4 924	1 357	1 331	69 736	27 325	2 945	17 936	27 262	152		
105 438	20	481	586	735	27 558	6 443	724	6 088	10 772	177		
47 934	11	20	12	24	0	18	0	12	10	84		
85 139	16	100	0	112	10	4	0	38	53	141		

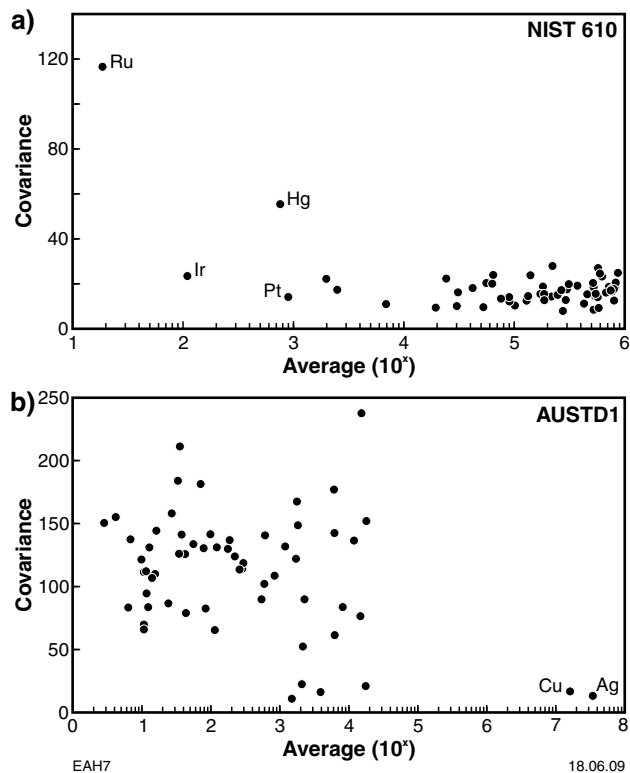


Figure 5. Plot of covariance versus average counts per second for Laser Ablation-Inductively Coupled Plasma-Mass Spectroscopy (LA-ICP-MS) of standard reference materials: a) Glass NIST 610; and b) Gold AUSTD1. The two standards were used as reference material for the Capricorn gold grain analyses; the elements labelled in part a) fall well below the proposed threshold value and should be considered the least reliable for this analysis, while the labelled elements in part b) are well above the threshold value and can be considered the most reliable.

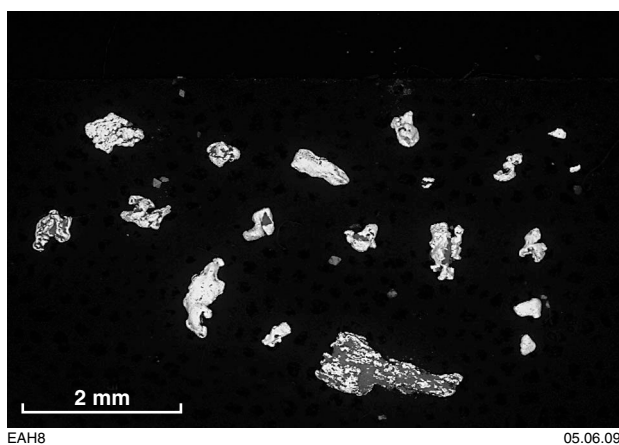


Figure 6. Scanning Electron Microscope Back-Scattered Electron image of alluvial gold from Hibernian, showing the variation in grain morphology.

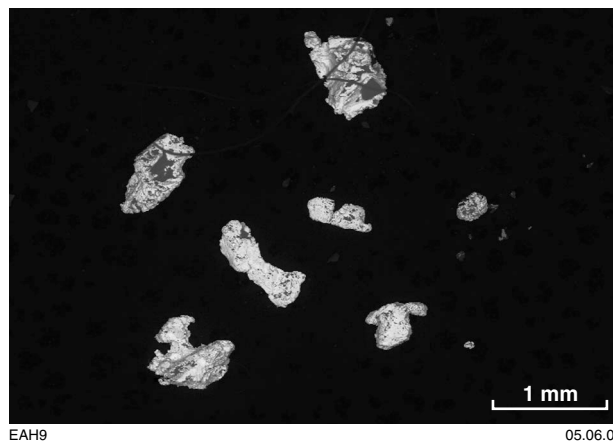


Figure 7. Scanning Electron Microscope Back-Scattered Electron image of Iode gold from Gaffney Find, showing the variation in grain morphology.

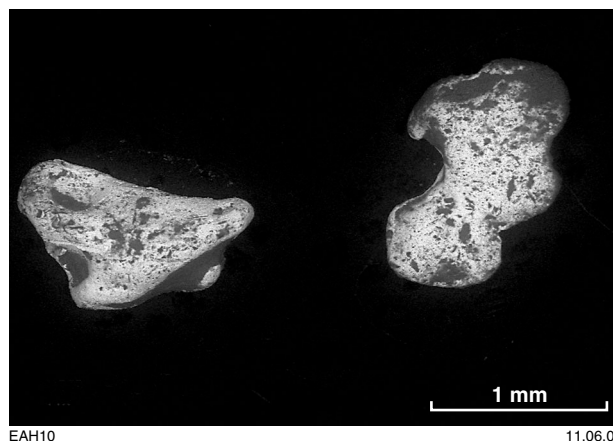


Figure 8. Scanning Electron Microscope Back-Scattered Electron image of well-rounded alluvial gold grains with pitted surface from Gaffney Find.

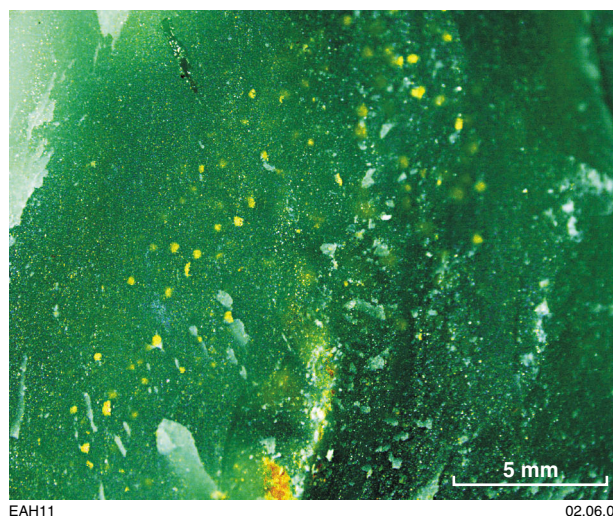
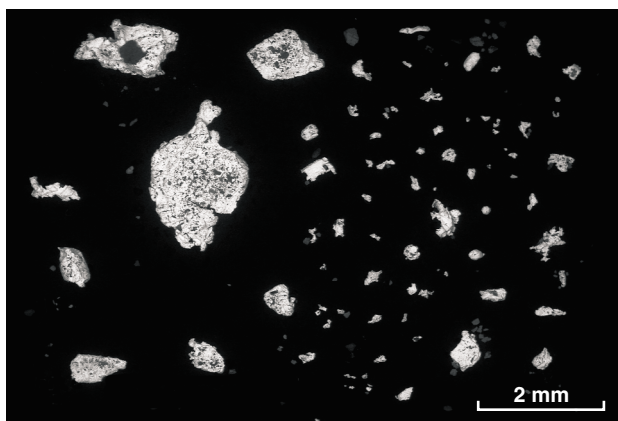
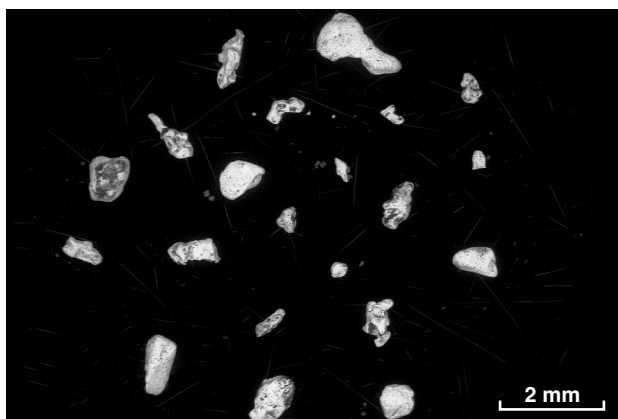


Figure 9. Distribution of gold flakes in variscite matrix from Low Hill. Reflected light; field of view 20 mm.



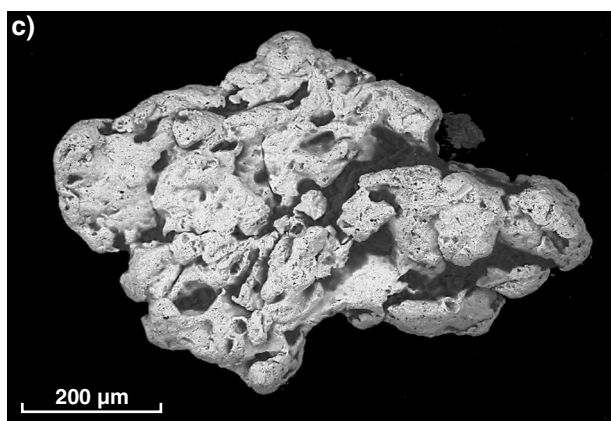
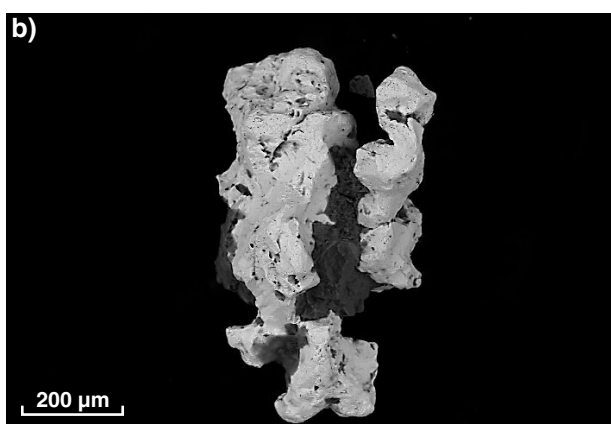
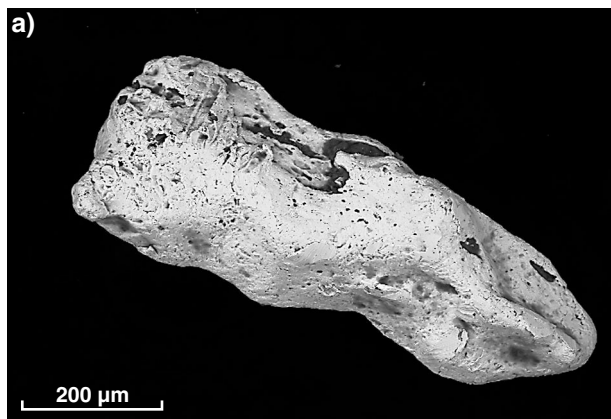
EAH12 05.06.09

Figure 10. Scanning Electron Microscope Back-Scattered Electron image of lode gold from Cobra, showing variation in grain morphology.



EAH13 11.06.09

Figure 11. Scanning Electron Microscope Back-Scattered Electron image of alluvial gold from McCarthys Patch, showing variation in grain morphology.



EAH14 11.06.09

Figure 12. Scanning Electron Microscope Back-Scattered Electron images showing the diversity of gold morphology from Hibernian: a) well-rounded grain with even surface; b) slightly rounded, semi-idiomorphic segregation with quartz and mica; c) medium-rounded lumpy grain.

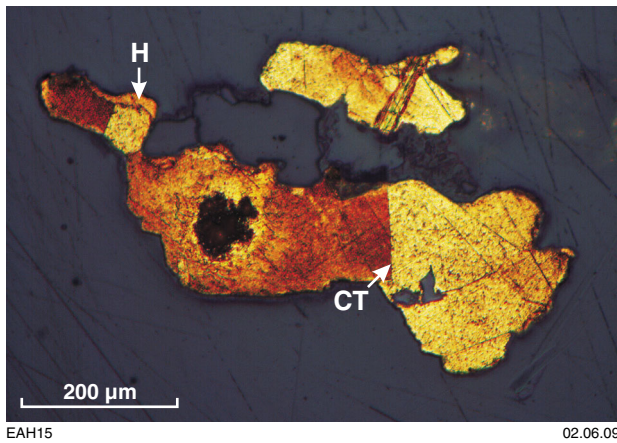


Figure 13. Internal structure of a Hibernian gold grain (0.7 mm length) showing coherent twin plane (CT) and high-purity segregations (H). Reflected light.

recrystallization, and high-purity segregations of probable secondary gold (Fig. 13). The other grains appear to be monocrystalline.

Gaffney Find

Gold in GSWA 149047 was recovered from weathered, brecciated, semi-translucent, brown-grey quartz. Other gangue minerals include barite, kaolinite, and mica. Apart from gold, no other metallic minerals were found in the vein.

Lode gold grains typically display irregular, cemented shapes (Fig. 7), but are more rounded than angular (Fig. 14), with pits and imprints from quartz grains on their uneven surface. Individual gold grains range in size from 0.1 to 0.9 mm, with a mean value of 0.7 mm.

The internal structure of one lode gold grain, revealed by etching in aqua regia, displays a partly recrystallized

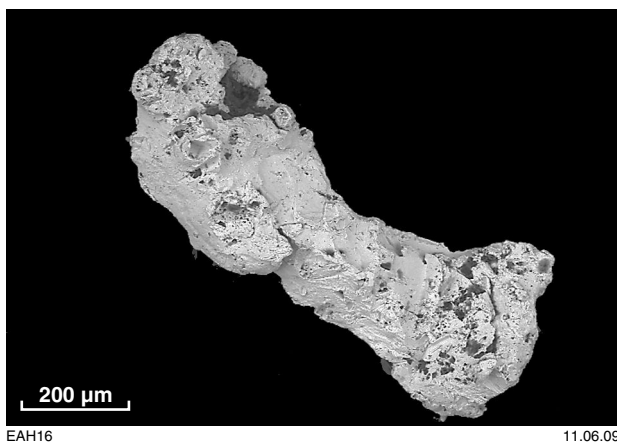


Figure 14. Scanning Electron Microscope Back-Scattered Electron image of solid, cemented lode gold grain from Gaffney Find.

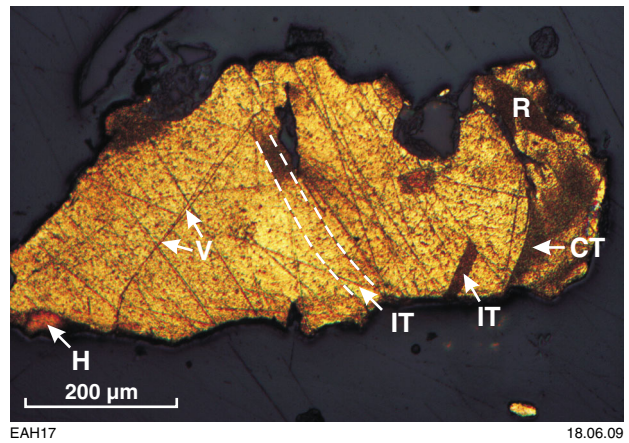


Figure 15. Internal structure of Gaffney Find lode gold grain (0.8 mm length) showing recrystallization (R), incoherent curved twin planes (IT), coherent curved twin plane (CT), intergranular veinlets (V), and a high-purity segregation (H). Reflected light

structure with curved coherent and incoherent twins, intergranular veinlets, and high-purity segregations of probable secondary gold (Fig. 15).

The two gold grains recovered from alluvium at Gaffney Find (Fig. 8) are large (1.3 and 1.6 mm), well-rounded, have even surfaces with grooves and scratches, and were probably originally lumpy or semi-idiomorphic in shape. Unfortunately these grains were lost during the mounting process, and could not be analysed.

Low Hill

The mineralogy of the variscite-hosted gold at Low Hill is described by Nickel et al. (2008). These authors note that gold was found within both cellular and massive variscite in a discordant variscite vein. However, the gold distribution is very irregular, with a few cells containing up to twenty gold particles, whereas most contain no gold. Gold in variscite can be divided into two categories: a) spongy or dendritic particles; and b) micron-sized, suspended particles and octahedral crystals. Spongy gold particles are up to 2 mm in size and disseminated throughout the translucent variscite, whereas dendritic gold is apparently concentrated along variscite grain boundaries.

Nickel et al. (2008) also recovered small amounts of gold at Low Hill by panning material from wallrock associated with variscite. This gold tends to be in solid particles, unlike the spongy gold recovered from the variscite itself. Some of the gold grains in this concentrate show abrasion markings, presumably due to the effects of transportation, although the separation process could also be responsible.

The gold analysed in the current project forms fine spongy films along variscite fissures and grain boundaries (Figs 9 and 16). The size of individual grains is up to 1 mm, and the gold is of high purity.

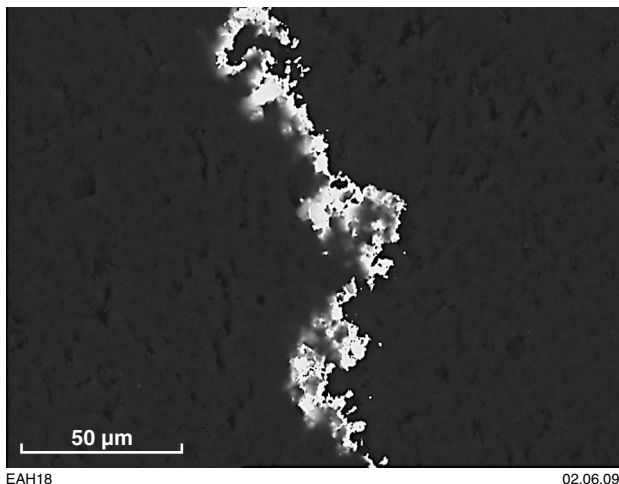


Figure 16. Scanning Electron Microscope Back-Scattered Electron image of spongy secondary gold in variscite at Low Hill. Transverse view.

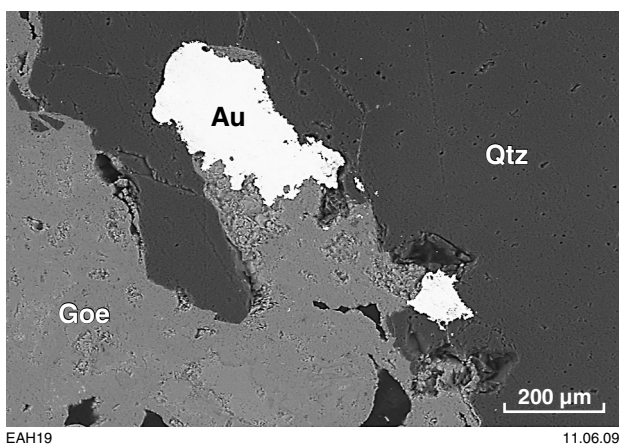


Figure 17. Scanning Electron Microscope Back-Scattered Electron image of a gold (Au), goethite (Goe), and quartz (Qtz) assemblage at Cobra.

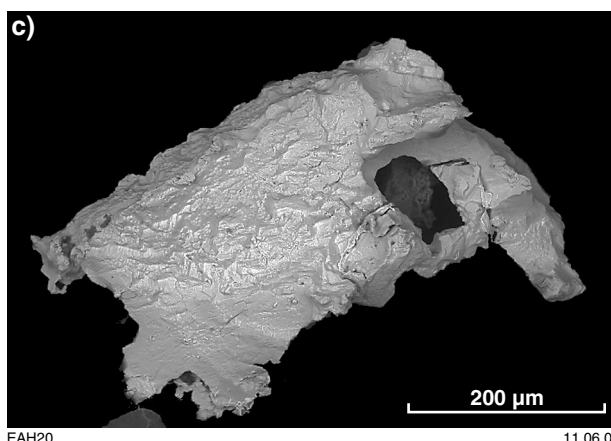
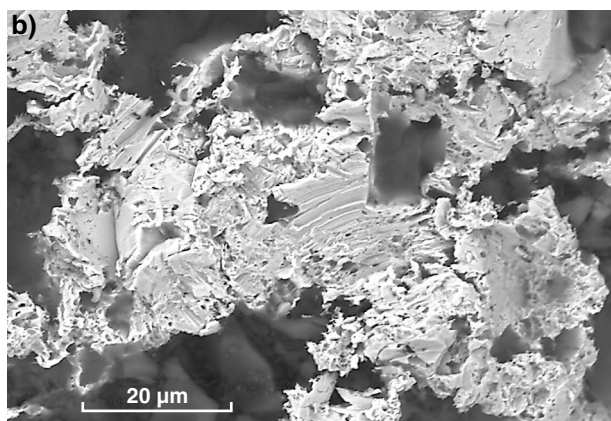
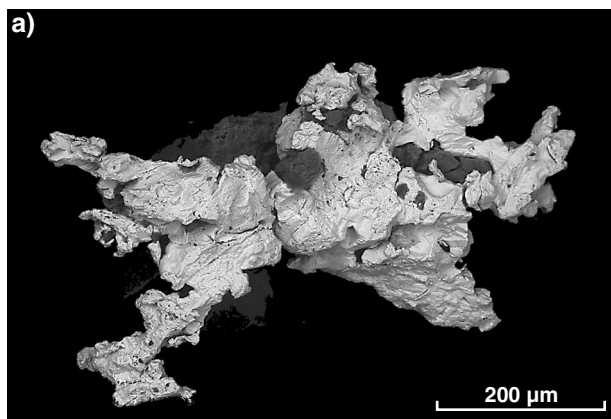


Figure 18. Scanning Electron Microscope Back-Scattered Electron image, showing variation in morphology of lode gold from Cobra: a) cemented lumpy and angular ('spider like') segregation with quartz and feldspar; b) scratched and pitted spongy grain surface; c) cellular and platy, smooth surface of a solid grain.

Bangemall MC

Cobra

Quartz vein material from Cobra is milky to opaque, with irregular veinlets of goethite and partly oxidized pyrite. Major cracks and fissures in the quartz are filled with copper and manganese oxides. Gold in the quartz vein is intergrown with goethite, and occurs along the boundary with quartz (Fig. 17).

Gold grains (Fig. 10) are angular, cemented, lumpy, and cellular (Fig. 18a) with some crystalline projections. Their surfaces are uneven, sometimes spongy and pitted (Fig. 18b), or cellular and platy (Fig. 18c). Some grains are intergrown with quartz and goethite. Individual grains range from less than 0.1 mm to 2.7 mm in size (mean 0.3 mm). Some zones of higher purity were observed in polished gold grains even before etching. They appear as marginal micrograins with straight boundaries (Fig. 19), and are more likely due to the initial recrystallization of grain margins than a result of leaching. The other high-purity zones form intergranular veinlets, likely a result of silver depletion (Hough et al., 2007) of the host gold grains at crystal boundaries (Fig. 20).

McCarthys Patch

Grains of alluvial gold from McCarthys Patch (Fig. 11) range in size from 0.4 to 1.8 mm (mean 0.9 mm), and are thus larger, and show less size variation, than gold grains from Cobra. Grains are well-rounded (Fig. 21), but some projections reveal originally semi-idiomorphic and cemented shapes. Grain surfaces are even and pitted, and are regularly associated with kaolinite, mica, and quartz grains.

Intergranular veinlets and irregular corrosive rims are typical of the internal structure of very high purity gold are typical of the internal structure of McCarthys Patch alluvial gold (Fig. 22). These are more pronounced compared with gold from Cobra. The

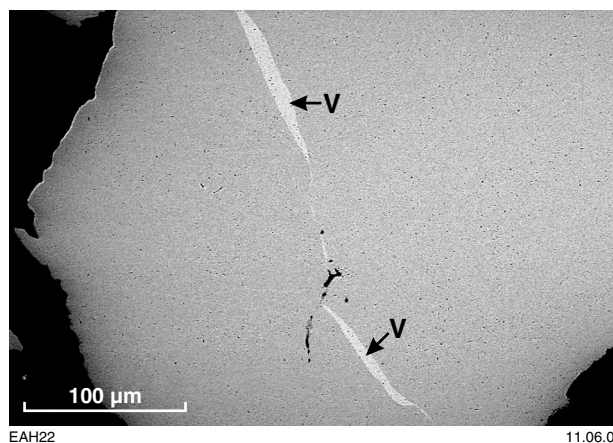


Figure 20. Scanning Electron Microscope Back-Scattered Electron image of the internal structure of lode gold grain from Cobra, showing high-purity intergranular veinlets (V).

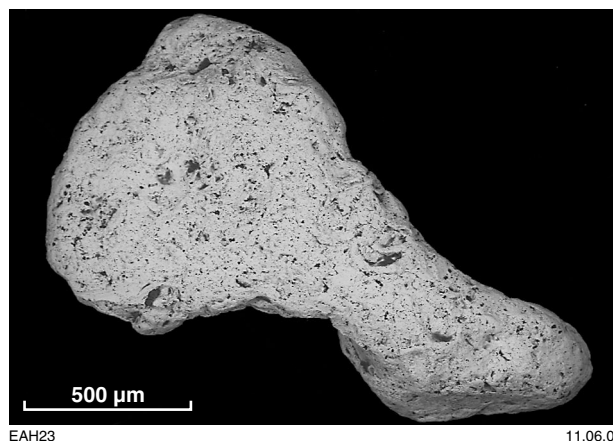


Figure 21. Scanning Electron Microscope Back-Scattered Electron image of a well-rounded lode gold grain with a pitted surface morphology, from McCarthys Patch.

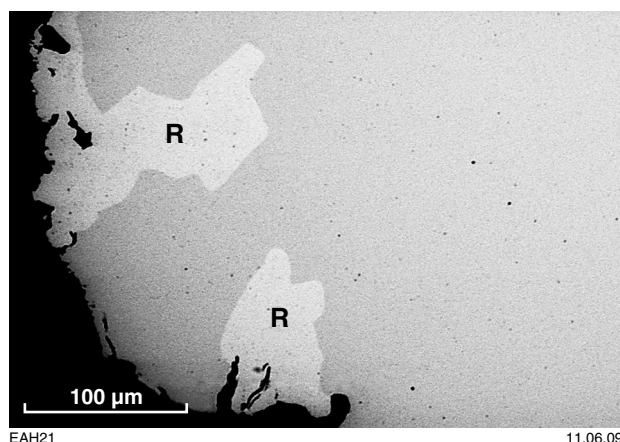


Figure 19. Scanning Electron Microscope Back-Scattered Electron image of a lode gold grain from Cobra, showing areas of initial recrystallization on the grain margin (R).

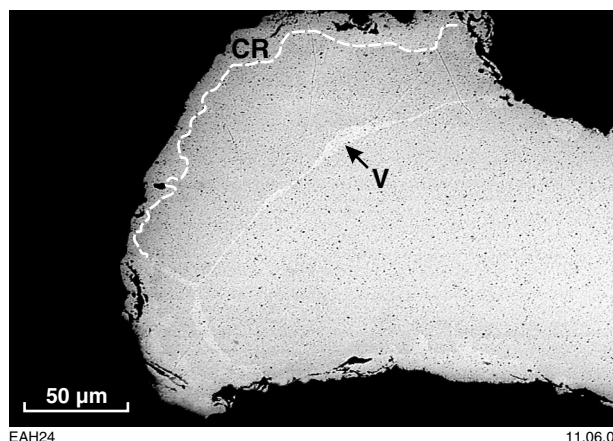


Figure 22. Scanning Electron Microscope Back-Scattered Electron image of the internal structure of an alluvial gold grain from McCarthys Patch, showing high-purity intergranular veinlets (V) and irregular corrosive rim (CR).

heavy fraction of McCarthys Patch alluvium also contains ilmenite, leucoxene, monazite, and rare zircon crystals.

Gold geochemistry

SEM-EDX results

The silver content of Egerton MC, Bangemall MC, and Low Hill gold was determined semi-quantitatively using SEM-EDX analyses. These results are summarized in Table 2.

Silver concentrations in Hibernian alluvial gold are consistently low, ranging from less than 0.5% in well-rounded grains, to 3% in less rounded particles. Vein-hosted gold from Gaffney Find shows similarly low levels, ranging from 2.5 to 4% Ag.

Variscite-hosted gold grains from Low Hill contain <0.5% Ag, the lowest concentration of any samples collected during this study.

Vein-hosted gold from the Cobra workings are characterized by a high silver concentration (9–19%, with a mean of 10.4%). Alluvial gold from McCarthys Patch shows limited variation in silver content, ranging from 5.6 to 7.8%. This limited variation in silver content can also be seen within each grain, if the high-purity intergranular veinlets and corrosive rims, and marginal micrograins (1–3% Ag) are excluded.

LA-ICP-MS results

The trace element signatures of bedrock and alluvial gold from the Egerton MC, Bangemall MC, and Low Hill were determined using LA-ICP-MS. Although two variscite chips from Low Hill containing films of spongy gold were also analysed, a trace element signature could not be determined due to high levels of aluminium, phosphorus, and other lithogenic elements, contaminants derived from the variscite and surrounding rocks.

Data from each mining centre is presented together in the form of spidergrams and XY plots. Principal Component Analysis has also been used to highlight any statistical grouping within the data.

Rapid visualization of variation within groups of elements can be made using spidergrams (e.g. Thompson et al., 1983). On this type of diagram (Fig. 23a–d), the concentration of each element is usually divided by that of a single composition. For example, in the treatment of basaltic rocks, it is common to normalize data to a mid-ocean ridge basalt (N-MORB) composition, or that of primitive mantle (Sun and McDonough, 1989). However, in this study, only raw count spiderdiagrams are presented, divided into siderophile (Ti, V, Cr, Mn, Fe, Co, Ni) and chalcophile (Cu, Zn, As, Mo, Ru, Rh, Pd, Ag, Cd, Sb, W, Re, Os, Bi) elements.

For chalcophile elements, all four spidergrams show similar forms. Copper and silver are above the 1000 cps

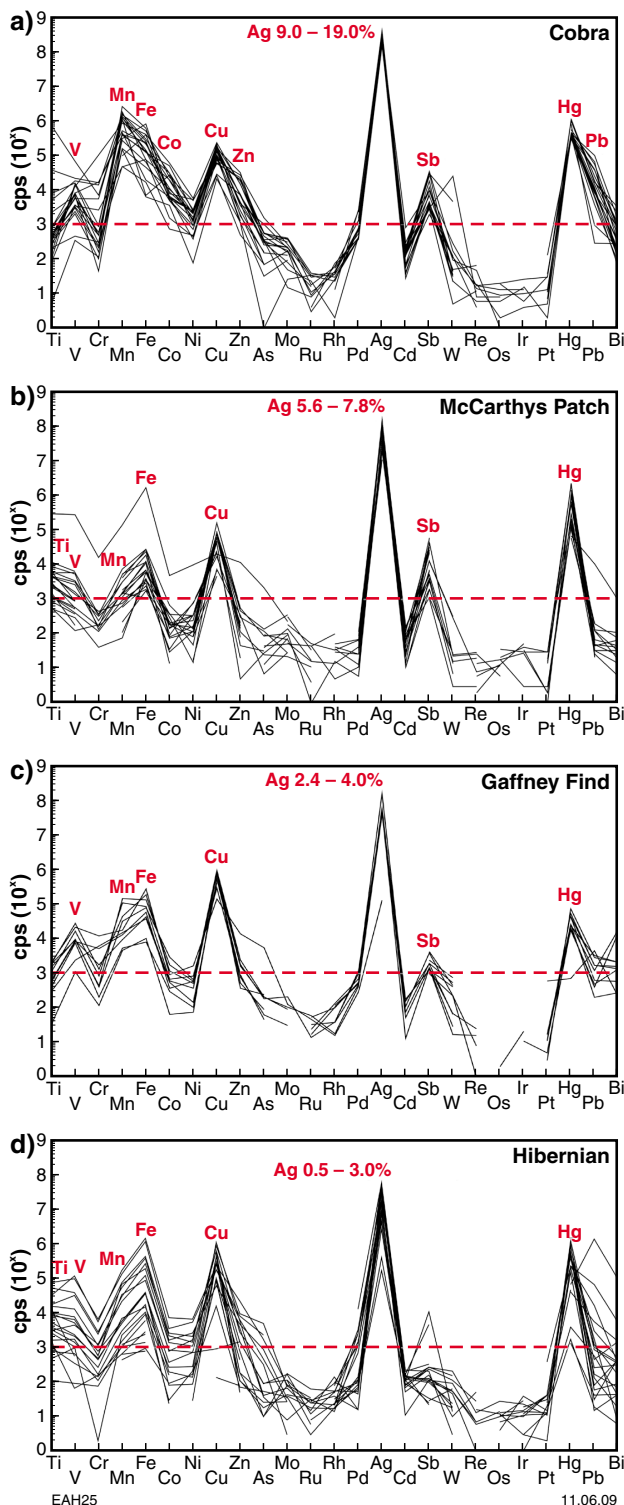


Figure 23. Spiderdiagrams showing the variations in siderophile (Ti–Ni) and chalcophile (Cu–Bi) elements for gold analysed by Laser Ablation-Inductively Coupled Plasma-Mass Spectroscopy (LA-ICP-MS, data in counts per second): a) Cobra lode gold (Bangemall MC); b) McCarthys Patch alluvial gold (Bangemall MC); c) Gaffney Find lode gold (Egerton MC); d) Hibernian alluvial gold (Egerton MC). Dashed lines at 1000 cps represents estimated upper level of background; percentage Ag values obtained by Scanning Electron Microscope with Energy Dispersive X-ray (SEM-EDX) analysis.

threshold for all grains analysed, and mercury is greater than, or close to, this 1000 cps threshold. Zinc, antimony, and lead are also above the threshold for some samples. There is a broad positive correlation of copper and silver for all groups (Fig. 24a). All but three analyses plot above the 1000 cps threshold for copper, and all silver results are well above this threshold. Relative to other gold grains analysed, alluvial and bedrock gold grains from the Egerton MC are generally elevated in copper, while gold grains from the Bangemall MC are generally elevated in silver. Within each mining centre, most alluvial gold grains have lower copper and silver concentrations than bedrock-hosted grains.

In terms of mercury and lead (Fig. 24b), the majority of analysed grains have >1000 cps Hg, but analyses are roughly equally divided above and below 1000 cps for lead. Most bedrock-hosted gold grains from the Bangemall MC have >1000 cps Pb, with values that are higher than those in alluvial gold grains from the same mining centre. Egerton (Gaffney Find) bedrock grains plot separately at lower mercury, and show limited overlap with Bangemall MC bedrock grains in terms of lead concentration. The alluvial grains from the Egerton MC largely plot with Bangemall MC alluvial grains.

The antimony content of both alluvial- and bedrock-hosted gold at the Bangemall MC (Fig. 24c) is similar, and weakly overlaps with bedrock-hosted gold grains from the Egerton MC. The remaining alluvial grains are relatively depleted in antimony, and some have lower mercury.

The behaviour of the siderophile elements, scandium, titanium, vanadium, chromium, manganese, iron, cobalt, and nickel (Fig. 23a–d), show that only iron and manganese are found at levels close to, or above, 1000 cps for all grains analysed. Vanadium, cobalt and nickel are also above 1000 cps for most Cobra bedrock gold grains (Fig. 23a), while vanadium is also higher in Gaffney Find bedrock gold grains (Fig. 23c). Manganese and iron (Fig. 25a) show a broad positive correlation for all gold grains, apart from Bangemall MC bedrock grains, which have notably higher manganese. Hibernian alluvial grains span the entire iron–manganese range, with most McCarthys Patch and Gaffney Find alluvial grains plotting at lower iron and manganese levels. The concentration of cobalt and vanadium show more scatter than iron and manganese (Fig. 25b), with most alluvial grains having lower cobalt and vanadium than bedrock grains. Bangemall MC bedrock grains plot at higher cobalt than other samples.

The behaviour of lithophile elements is less easy to interpret, as most elements plot at less than threshold values.

Principal Components Analysis

Principal Components Analysis (PCA) is a powerful statistical technique used to determine patterns in multivariate datasets (Davis, 1973). It involves the projection of multivariate observations onto new orthogonal axes, termed principal components, which are linear combinations of the original variables. The principal

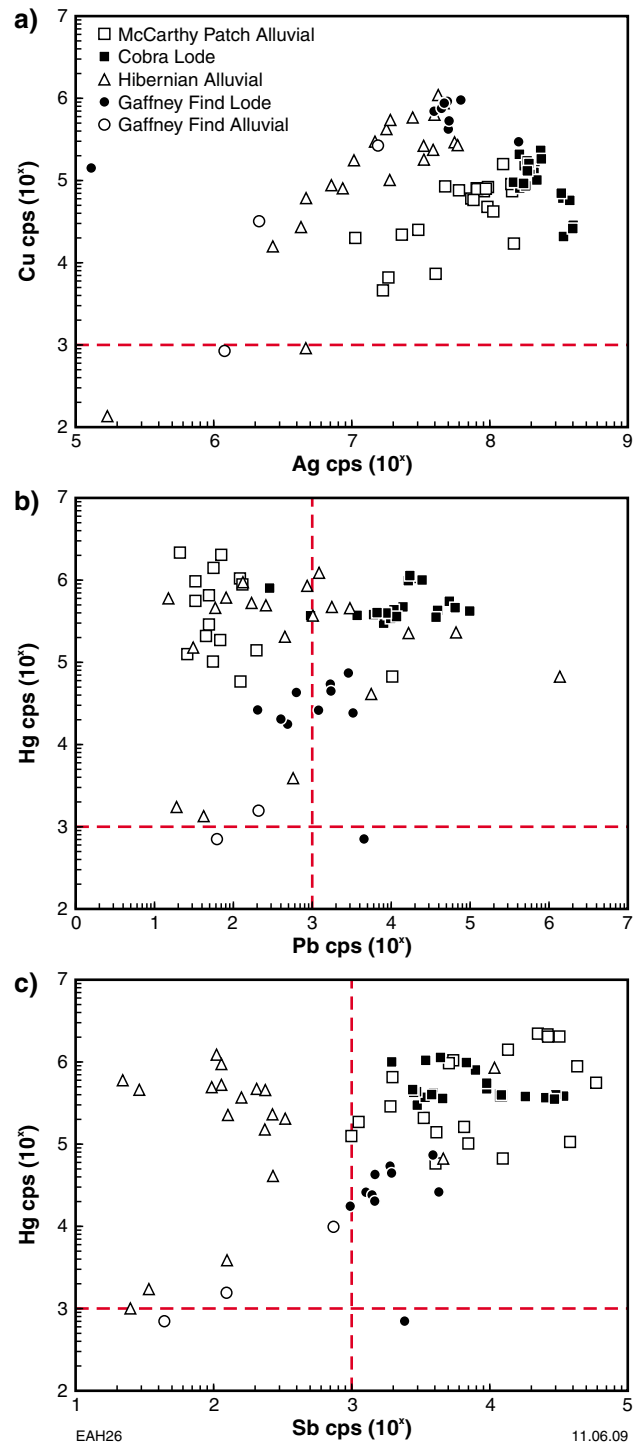


Figure 24. Bivariate element plots (all Capricorn gold samples) showing variation in: a) silver versus copper; b) lead versus mercury; and c) antimony versus mercury. Data from Laser Ablation-Inductively Coupled Plasma-Mass Spectroscopy (LA-ICP-MS) in counts per second. Dashed lines at 1000 cps represent estimated upper level of background.

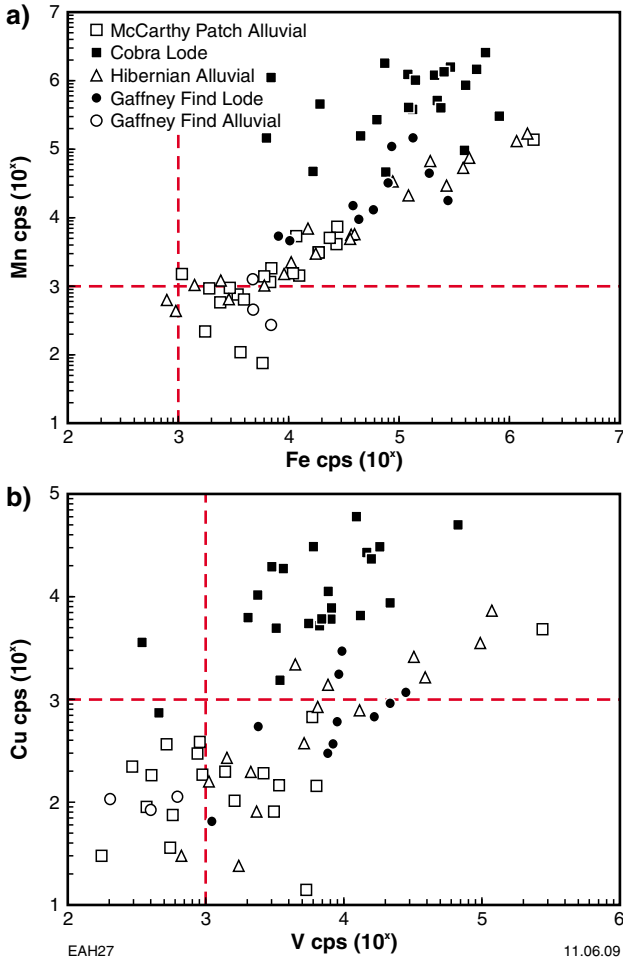


Figure 25. Bivariate element plots (all Capricorn gold samples) showing variation in: a) iron versus manganese; and b) vanadium versus cobalt. Data from Laser Ablation-Inductively Coupled Plasma-Mass Spectroscopy (LA-ICP-MS) in counts per second. Dashed lines at 1000 cps represent estimated upper level of background.

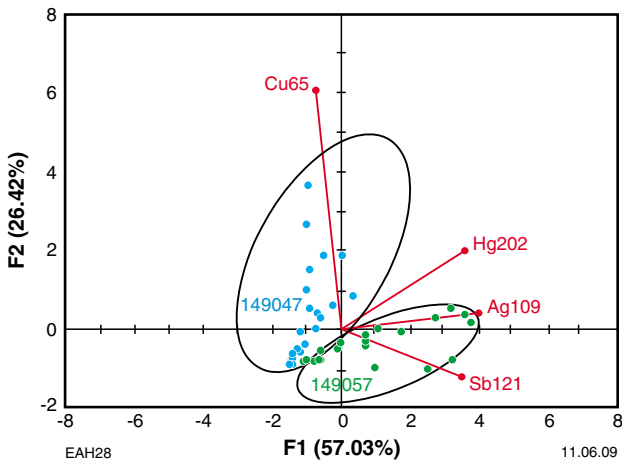


Figure 26. Principal Components Analysis for the sample series 149047 and 149057, based on copper, silver, antimony, and mercury.

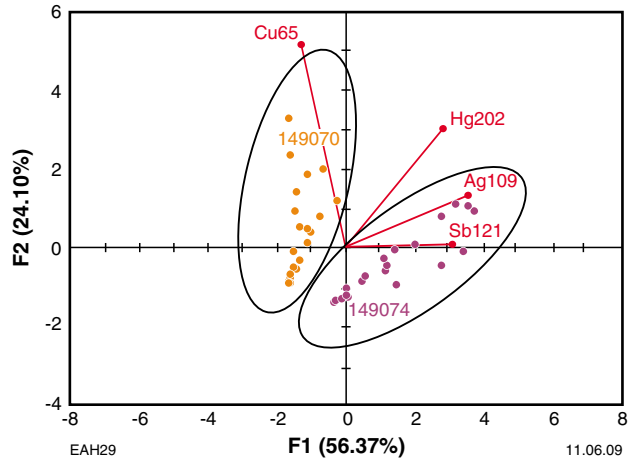


Figure 27. Principal Components Analysis for the sample series 149070 and 149074, based on copper, silver, antimony, and mercury.

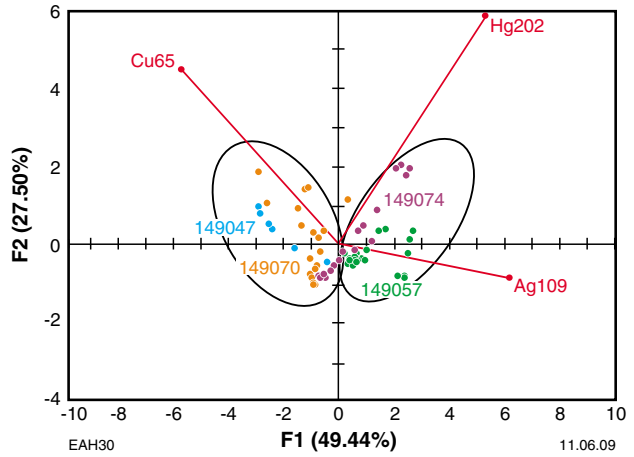


Figure 28. Principal Components Analysis for the complete Capricorn sample series, based on copper, silver, and mercury.

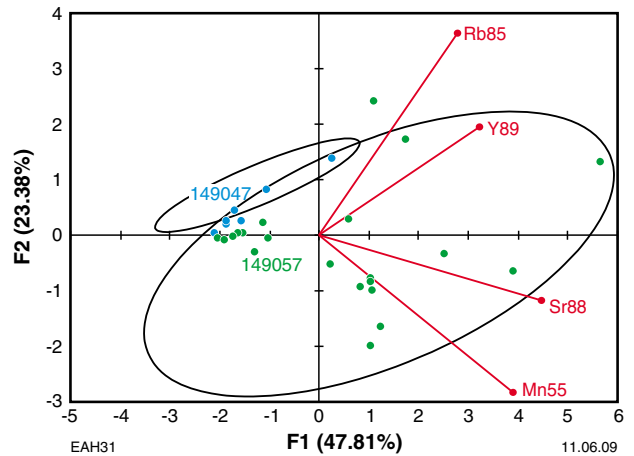


Figure 29. Principal Components Analysis for the sample series 149047 and 149057, showing differences between lithogenic elemental associations for the two sets of data. Separation is based on rubidium, yttrium, strontium, and manganese.

components are thus the eigenvectors of the variance-covariance matrix (Neuendorf et al., 2005).

A PCA plot of the elements copper, silver, antimony, and mercury from bedrock samples 149047 (Gaffney Find) and 149057 (Cobra) shows that the two sets of samples represent discrete populations derived from different geological environments (Fig. 26).

When data from alluvial samples 149070 (Hibernian) and 149074 (McCarthy's Patch), are compared using a similar PCA plot for copper, silver, antimony, and mercury (Fig. 27), there is again sufficient individuality in the two subgroups to indicate the lack of co-provenance of the two datasets, although there is some degree of overlap of the two PCA fields.

When the entire dataset is plotted on the same graph (Fig. 28), using copper, silver, and mercury as primary components of a PCA series, an association can be observed between the Bangemall MC sample series (149074 and 149057) and the Egerton MC series (149070 and 149047), with only a single analysis being slightly removed from the two groups. This association can only be seen for the three elements mentioned, and it is difficult to see any other interelement relationships using PCA.

The lithophile isotopes (Fig. 29) from bedrock samples 149047 (Gaffney Find) and 149057 (Cobra) provide some evidence that the two series have been derived from different host rocks. Although there is a significant vector in a PCA plot using rubidium, yttrium, strontium, and manganese, this distinction is not totally convincing, and any interpretation based on this result needs to be treated with caution.

Discussion

Results presented here show that there is significant regional variation in gold mineralogy and trace element chemistry within the Capricorn Orogen, and that this variation is reflected in both bedrock-hosted and alluvial gold. The study also indicates that while bedrock-hosted and alluvial gold from the same area are broadly similar in terms of mineralogy and chemistry, they display important differences, most likely as a result of weathering and transport processes. The effects of weathering are not confined to samples of alluvial gold, with outcrop specimens of bedrock-hosted gold also showing evidence of weathering in the form of mineralogical changes and trace element depletion, a factor that has to be borne in mind when assessing the chemistry of potential source rocks and mineralizing fluid systems.

Regional variation in gold mineralogy and chemistry

Egerton MC

Both bedrock-hosted and alluvial gold from the Egerton MC can be distinguished from Bangemall MC gold through their low silver concentrations, high copper

to silver ratios, low mercury to lead ratios, and the presence of recrystallized twinning with some high-purity segregations. This separation is also shown through PCA results based on copper, silver, antimony, and mercury concentrations.

The presence of incoherent twins and deformed twin lamellae in the crystal structure of Egerton gold points to the presence of thermal recrystallization during an early metamorphic event. This metamorphism could also have caused the depleted silver levels seen within Egerton gold; however, the occurrence of weathered, unmineralized quartz in association with low-silver primary gold, and the possibility of secondary gold adhesions at this location, is more suggestive of depletion due to weathering at the lower saprolite level of a lateritic profile (Freyssinet et al., 2005). Under these weathering conditions, recrystallization of gold grains and bending of pre-existing twin lamellae may also have occurred due to mechanical deformation (Petrovskaya, 1973). This possible interpretation of high-purity segregations as secondary in turn suggests remobilization and redeposition of gold under arid climatic conditions and the influence of saline fluid movement (Freyssinet et al., 2005).

Based on the wide variation in gold morphology and trace element chemistry, at least two populations of alluvial gold are present at Hibernian. These could be derived from separate sources, with the gold either introduced at the same time or during different periods. The two grains of alluvial gold obtained from Gaffney Find have endured a long history of mechanical, and possibly even metamorphic, alteration, and therefore could not be compared to the quartz vein gold at their locality. The very low trace element levels in these two alluvial grains also hampered comparisons with gold from other sources.

Low Hill

Gold associated with variscite at Low Hill has a distinctive morphology and very high purity, quite unlike gold from either the Egerton or Bangemall mining centres. Textural evidence also indicates that the gold and variscite are co-precipitates.

Nickel et al. (2008) showed that spongy gold flakes in variscite from Low Hill were formed by the remobilization and redeposition of stratiform gold by low-temperature, saline hydrous solutions in a supergene environment. Both spongy and dendritic gold are thus secondary in origin, and could have formed at the same time as the high-purity segregations in Egerton MC gold.

Bangemall MC

Bedrock-hosted and alluvial gold from the Bangemall MC differs from Egerton MC gold in its association with pyrite and milky quartz, higher silver content, and relatively simple, monocrystalline internal structure. In terms of trace element chemistry, bedrock-hosted and alluvial gold grains are characterized by higher silver to copper ratios, and have higher mercury and antimony levels, respectively, than their Egerton MC equivalents. These

features indicate the primary hypogene mineralization occurred in a shallow, slightly oxidized environment, rather than in a deeper crustal setting. Later supergene alterations are expressed by the formation of high-purity veinlets, and corrosive rims.

Small variations in size, roundness, silver content, and trace element distribution indicate a single original source for the McCarthys Patch alluvial gold grains. This source is likely to be similar to the quartz- and pyrite-veined host rocks present at the Cobra workings; however, the high degree of rounding and depleted trace element chemistry of the alluvial gold suggests either transport over a considerable distance, or excessive weathering. Therefore, although the sample location is less than a kilometre from the local drainage watershed, the alluvial gold may originally have been sourced from outside the present drainage system; alternately, it may have been subject to several periods of reworking and weathering. Support for the latter idea can be seen in the work of Martin et al. (2005), who noted that the northern Capricorn Orogen has experienced at least three major cycles of alluvial sedimentation during the Cenozoic.

Gold mineralization history

The results presented here suggest that the western Capricorn Orogen underwent at least two separate gold mineralization events during the Proterozoic. Locally, these events were followed by a period of gold remobilization and secondary gold deposition under supergene conditions, which probably took place some time during the Phanerozoic.

The Egerton MC gold is hosted by low-grade metasedimentary and metamorphosed mafic igneous rocks that have been correlated with the 2.0–1.65 Ga old Padbury Group. Although age constraints are poor, it is clear from comparison with other similarly aged rocks in the Capricorn Orogen that the host rocks have experienced a protracted history of deformation and metamorphism from the Paleoproterozoic to Neoproterozoic. Gold from the Egerton MC reflects this complex geological history, being characterized by relatively high-pressure and high-temperature mineralogy, and a complex history of recrystallization. The formation of the high-purity secondary gold segregations present in lode and alluvial gold at the Egerton MC probably occurred during the Phanerozoic as a result of gold remobilization and redeposition caused by the interaction of saline groundwater with the products of earlier lateritic weathering (Freyssinet et al., 2005).

In contrast, gold mineralization at the Bangemall MC is hosted by Edmondian age (1030 to 950 Ma) quartz veins in the Edmund Group and Narimbunna Dolerite. Both the host rocks and quartz veins have experienced only low-grade metamorphism, followed by further, relatively minor deformation during the 570 Ma Mulka tectonic event (Bodorkos and Wingate, 2007; Johnson et al., 2009). The geological history of the host rocks is also reflected in the mineralogy and chemistry of the gold, which indicates formation at relatively low-pressure and

low-temperature conditions, and insignificant subsequent hypogenic recrystallization. Secondary gold is not present at the Bangemall MC, suggesting that the original gold chemistry and mineralogy has been only slightly modified by Phanerozoic weathering.

Gold associated with variscite at Low Hill is distinct from both the Bangemall and Egerton MC deposits. It is a secondary deposit that resulted from the remobilization of gold during a low-temperature hydrothermal event post-dating the Edmondian Orogeny, and probably also post-dating the Mulka tectonic event (Nickel et al., 2008).

Conclusions

This study is the first time that gold mineralogy and trace element chemistry has been used to compare gold deposits, and improve the understanding of mineralization events in the Capricorn Orogen. The main findings are:

- Gold from the Egerton and Bangemall mining centres has a primary origin, contrasting with the secondary nature of gold at Low Hill;
- Differences in gold mineralogy and chemistry between the Egerton and Bangemall mining centres reflect separate geological settings, and complex metamorphic and weathering histories;
- There were at least two periods of hydrothermal gold mineralization during the Proterozoic, and at least one period of secondary gold formation during the Phanerozoic;
- Gold was co-precipitated with quartz at the Bangemall and Egerton mining centres, and with variscite at Low Hill. However, in both cases the gold was deposited last, filling spaces between quartz grains, and within variscite fissures;
- Alluvial gold from Hibernian in the Egerton Mining Centre was derived from several sources, but is similar to bedrock-hosted gold from the nearby Gaffney Find workings;
- Alluvial gold from McCarthys Patch in the Bangemall Mining Centre was derived from a single source similar to bedrock-hosted gold from the nearby Cobra deposit, and has likely undergone several transport cycles before being incorporated into the present-day alluvial sediment.

Acknowledgements

The authors wish to thank Michael Verrall for his help in operating the SEM at CSIRO; Jim Miller and David Vaughan for the supply of material from Bangemall Mining Centre and Low Hill respectively; David Vaughan for the preparation of polished slabs; Alan Thomas and Cameron Scadding (UWA) for the LA-ICP-MS analysis; Robert Hough (CSIRO) for his constructive manuscript review; and Derek Winchester (CSIRO) for the preparation of gold sections.

References

- Blockley, JG 1971, The lead, zinc and silver deposits of Western Australia: Geological Survey of Western Australia, Mineral Resources Bulletin 9, 234p.
- Bodorkos, S and Wingate, MTD 2007, The contribution of geochronology to GSWA's mapping programs: current perspectives and future directions: Geological Survey of Western Australia, Record 2007/2, p. 10–11
- Boyle, RW 1979, The geochemistry of gold and its deposits: Canadian Geological Survey, Bulletin 280, 584p.
- Brooklea Geoservices 1998, Report on exploration for the year ending 31/12/1998, Egerton Project, EL52/790, PL52/764, ML52/343, and ML52/567; Egerton Gold NL: Geological Survey of Western Australia, Statutory mineral exploration report, A53867 (unpublished).
- Cawood, PA and Tyler, IM 2004, Assembling and reactivating the Proterozoic Capricorn Orogen: lithotectonic elements, orogenies, and significance: *Precambrian Research*, v. 128, p. 201–218.
- Chapman, RJ, Leake, RC and Styles, M 2002, Microchemical characterization of alluvial gold grains as an exploration tool: *Gold Bulletin*, v. 35, no. 2, p. 53–65.
- Cooper, RW, Langford, RL and Pirajno, F 1998, Mineral occurrences and exploration potential of the Bangemall Basin: Geological Survey of Western Australia, Report 64, 42p.
- Dahl, N 1997, Annual report for Exploration Licences 521790, 52/843, 52/913-917, 52/919, 52/952, 52/972, Prospecting Licence 521764 and Mining Leases 52/343 and 52/567, Egerton Project; Egerton Gold NL: Geological Survey of Western Australia, Statutory mineral exploration report, A50956 (unpublished).
- Davis, JC 1973, *Statistics and data analysis in geology*: John Wiley and Sons Inc., New York, USA, 550p.
- Freyssinet, P, Butt, CRM, Morris, RC and Piantone, P 2005, Ore-forming processes related to lateritic weathering, in *Economic Geology one hundredth anniversary volume 1905–2005*: Society of Economic Geologists Inc, Littleton, Colorado, USA, p. 681–722.
- Gee, RD 1979, Structure and tectonic style of the Western Australian Shield: *Tectonophysics*, v. 58, p. 327–369.
- Gee, RD 1990, Nabberu Basin, in *Geology and mineral resources of Western Australia*: Geological Survey of Western Australia, Memoir 3, p. 202–210.
- Hassan, LY 2007, Mineral occurrences and exploration activities of the Gascoyne area: Geological Survey of Western Australia, Record 2007/17.
- Hough, RM, Butt, CRM, Reddy, SM and Verrall, M 2007, Gold nuggets: supergene or hypogene? *Australian Journal of Earth Sciences*, v. 54, p. 959–964.
- Johnson, SP, Sheppard, S, Rasmussen, B, Muhling, JR, Fletcher, IR, Wingate, MTD, Kirkland, CL and Pirajno, F 2009, Meso- to Neoproterozoic reworking in the Gascoyne Complex and what it means for mineral exploration: Geological Survey of Western Australia, Record 2009/2, p. 23–25.
- Kinny, PD, Nutman, AP and Occhipinti, SA 2004, Reconnaissance dating of events recorded in the southern part of the Capricorn Orogen: *Precambrian Research*, v. 128 no. 3–4, p. 279–294.
- Knight, JB, Morrison, SR and Mortensen, JK 1999, The relationship between placer gold particle shape, rimming, and distance of fluvial transport as exemplified by gold from the Klondike District, Yukon Territory, Canada: *Economic Geology*, v. 94, p. 635–648.
- Krapez, B 1999, Stratigraphic record of an Atlantic-type global tectonic cycle in the Palaeoproterozoic Ashburton Province of Western Australia: *Australian Journal of Earth Sciences*, v. 46, no. 1, p. 71–87.
- Martin, DMcB and Thorne, AM 2004, Tectonic setting and basin evolution of the Bangemall Supergroup in the northwestern Capricorn Orogen: *Precambrian Research*, v. 128, p. 385–409.
- Martin, DMcB, Sheppard, S and Thorne, AM 2005, Geology of the Maroonah, Ullawarra, Capricorn, Mangarooon, Edmund, and Elliott Creek 1:100 000 sheets: Geological Survey of Western Australia, 1:100 000 Geological Series Explanatory Notes, 65p.
- Martin, DMcB, Sheppard, S, Thorne, AM, Farrell, TR and Groenewald, PB 2006, Proterozoic geology of the northwestern Capricorn Orogen — a field guide: Geological Survey of Western Australia, Record 2006/18, 43p.
- Muhling, PC, Brakel, AT and Davidson, WA 1978, Mount Egerton, W.A.: Geological Survey of Western Australia, 1:250 000 Geological Series Explanatory Notes, 28p.
- Myers, JS 1993, Precambrian history of the West Australian Craton and adjacent orogens: *Annual Review of Earth and Planetary Sciences*, v. 21, p. 453–485.
- Nickel, EH, Hough, R, Verrall, MH, Hancock, E, Thorne, AM and Vaughan, D 2008, The Woodlands variscite-gold occurrence in the north Gascoyne region of Western Australia: *Australian Journal of Mineralogy*, v. 14, June, p. 27–36.
- Nikolaeva, LA, Gavrillov, AM, Nekrasova, AN, Yablokova, SV and Shatilova, LV 2004, Native gold in lode and placer deposits of Russia, in *Atlas: TsNIGRI, Moscow, Russia*, 176p.
- Neuendorf, KKE, Mehl, JP and Jackson, JA 2005, *Glossary of geology (5th Edition)*: American Geological Institute, Alexandria, USA, 779p.
- Occhipinti, SA, Swager, CP and Pirajno, F 1996, Structural and stratigraphic relationships of the Padbury Group, Western Australia — implications for tectonic history: Geological Survey of Western Australia, *Annual Review 1995–96*, p. 88–95.
- Occhipinti, SA, Sheppard, S, Myers, JS, Tyler, IM and Nelson, DR 2001, Archaean and Palaeoproterozoic geology of the Narryer Terrane (Yilgarn Craton) and the southern Gascoyne Complex (Capricorn Orogen), Western Australia — a field guide: Geological Survey of Western Australia, Record 2001/8, 78p.
- Occhipinti, SA, Sheppard, S, Passchier, C, Tyler, IM and Nelson, DR 2004, Palaeoproterozoic crustal accretion and collision in the southern Capricorn Orogen: the Glenburgh Orogeny: *Precambrian Research*, v. 128, no. 3–4, p. 237–255.
- Petrovskaya, NV 1973, *Native Gold*: Nauka, Moscow, Russia, 347p. (in Russian).
- Pirajno, F, Bagas, L, Swager, CP, Occhipinti, SA and Adamides, NG 1996, A reappraisal of the stratigraphy of the Glengarry Basin, Western Australia: Geological Survey of Western Australia, *Annual Review 1995–96*, p. 81–87.
- Sheppard, S 2004, Unravelling the complexity of the Gascoyne Complex: Geological Survey of Western Australia, Record 2004/5, p. 26–28.
- Sheppard, S and Swager, CP 1999, Geology of the Marquis 1:100 000 sheet: Geological Survey of Western Australia, 1:100 000 Geological Series Explanatory Notes, 21 p.
- Sheppard, S, Occhipinti, SA and Nelson, DR 2005, Intracontinental reworking in Capricorn Orogen, Western Australia: the 1680–1620 Ma Mangarooon Orogeny: *Australian Journal of Earth Sciences*, v. 52, no. 3, p. 443–460.
- Sheppard, S, Farrell, TR, Martin, DMcB, Thorne, AM and Bagas, L 2008, Mount Phillips, WA Sheet 2149: Geological Survey of Western Australia, 1:100 000 Geological Series.
- Sun, S-s and McDonough, WF 1989, Chemical and isotopic systematics of oceanic basalts: implications for mantle composition and processes, in *Magmatism in the Ocean Basins edited by AD Saunders and MJ Norry*: Geological Society Special Publication, no. 42, p. 313–345.

- Swager, CP and Myers, JS 1999, Geology of the Milgun 1:100 000 sheet: Geological Survey of Western Australia, 1:100 000 Geological Series Explanatory Notes, 27p.
- Thompson, RN, Morrison MA, Dickin AP and Hendry GL 1983, Continental flood basalts...Arachnids rule OK? *In* Continental basalts and mantle xenoliths *edited by* CJ Hawkesworth and MJ Norry: Shiva Publishing Ltd, UK, p. 158.
- Tyler, IM and Thorne, AM 1990, The Northern Margin of the Capricorn Orogen, Western Australia — an example of an Early Proterozoic Collision Zone: *Journal of Structural Geology*, v. 12, no. 5–6, p. 685–701.
- Watling, RJ, Herbert, HK, Delev, D and Abell, ID 1994, Gold fingerprinting by laser ablation inductively coupled plasma mass spectrometry: *Spectrochimica Acta*, v. 49B, no. 2, p. 205–219.
- Williams, SJ, Williams, IR, Chin, RJ, Muhling, PC and Hocking, RM 1983, Mount Phillips, WA: Geological Survey of Western Australia, 1:250 000 Geological Series Explanatory Notes, 29p.

Appendix

Laser Ablation (LA-ICP-MS) analysis

Laser Ablation-Inductively Coupled Plasma-Mass Spectrometry (LA-ICP-MS) analysis involves focusing the laser at a point on the surface of a sample, causing the ionization of the argon carrier gas that surrounds the sample. The resulting plasma volatilizes the sample through thermal conduction. This volatilized material is then ionized, with ionic species identified in terms of their mass-to-charge ratio. Due to several factors (including matrix effects), the resulting data are only semi-quantitative, and are reported here as counts per second (cps).

All measurements were carried out using an Agilent 7500CS ICP-MS system, located in the Forensic Laboratory, The University of Western Australia, Crawley. Samples were ablated using a 213 nm New Wave UP213 laser ablation unit (New Wave, Fremont, CA). Instrumental settings were optimized using a NIST 610 glass standard, a procedure that was repeated daily to ensure between-batch comparison of data, and to facilitate drift normalization. Samples were ablated, where possible, for 30 seconds at 10 Hz, with a laser energy of 55%, fluence of 32 J/cm², and spot size of 50 µm. For some gold grains, only two or three analyses could be made, as the material was too small and thin, leading to rapid consumption of the sample.

Analytical results, and analyses of two reference materials (NIST 610 and AUSTD1), are shown in Table 4, along with calculations of the mean and covariance (i.e. 100SD/mean).

This Record is published in digital format (PDF) and is available online at:
www.dmp.wa.gov.au/GSWApublications.
Laser-printed copies can be ordered from the Information Centre for the
cost of printing and binding.

Further details of geological publications and maps produced by the
Geological Survey of Western Australia can be obtained by contacting:

Information Centre
Department of Mines and Petroleum
100 Plain Street
EAST PERTH, WESTERN AUSTRALIA 6004
Phone: (08) 9222 3459 Fax: (08) 9222 3444
www.dmp.wa.gov.au/GSWApublications

